HOKKAIDO UNIVERSITY

Title	Effectiveness of pulse dosing of submicron super-fine powdered activated carbon in preventing transmembrane pressure rise in outside-in-type tubular and inside-out-type monolithic ceramic membrane microfiltrations
Author(s)	Zhao, Yuanjun; Matsui, Yoshihiko; Saito, Shun et al.
Citation	Separation and Purification Technology, 296, 121403 https://doi.org/10.1016/j.seppur.2022.121403
Issue Date	2022-09-01
Doc URL	https://hdl.handle.net/2115/93025
Rights	© 2022. This manuscript version is made available under the CC-BY-NC-ND 4.0 license http://creativecommons.org/licenses/by-nc-nd/4.0/
Rights(URL)	https://creativecommons.org/licenses/by-nc-nd/4.0/
Type	journal article
File Information	SEPPUR_121403.pdf

Hokkaido University Collection of Scholarly and Academic Papers : HUSCAP

Effectiveness of pulse dosing of submicron super-fine powdered activated carbon in preventing transmembrane pressure rise in outside-in-type tubular and inside-out-type monolithic ceramic membrane microfiltrations

Yuanjun Zhao [a], *Yoshihiko Matsui* [b,*], *Shun Saito* [a], *Nobutaka Shirasaki* [b], *Taku Matsushita* [b]

[a] *Graduate School of Engineering, Hokkaido University, N13W8, Sapporo, 060-8628, Japan*

[b] *Faculty of Engineering, Hokkaido University, N13W8, Sapporo, 060-8628, Japan*

* *Corresponding author*. Tel/fax: +81-11-706-7280

E-mail address: matsui@eng.hokudai.ac.jp (Y. Matsui)

ABSTRACT

Membrane fouling is still a major problem in water treatment that uses membrane separation. In this study, submicron-sized super-fine powdered activated carbon (SSPAC) was applied in a pulse/continuous dose to ceramic-membrane microfiltrations of two very different types: a submerged tubular membrane system that enabled vacuum-driven, outside-in filtration and a monolithic membrane system that enabled pressure-driven, inside-out filtration. Constant-flux filtration with repeated hydraulic backwashing was performed using diluted secondary-treated municipal wastewater and natural river water, and the effect and mechanism of membrane fouling mitigation were investigated. Pulse dosing with SSPAC alleviated a rise of transmembrane pressure (TMP) more than continuous dosing in the submerged tubular membrane system because of the effects, inter alia, associated with precoating the SSPAC layer as well as adsorption, by which soluble membrane foulants were effectively removed. Moreover, pulse-dosed SSPAC combined with a coagulant formed a precoat layer on the membrane that was easy to peel off with hydraulic backwashing. Continuous dosing of SSPAC was inferior to pulse dosing of SSPAC in terms of water quality, and some SSPAC was left on the membrane surface after hydraulic backwashing. In the monolithic membrane system, however, the superiority of pulse dosing of SSPAC was not observed: pulse and continuous dosing of SSPAC led to similar reductions of TMP rise. The SSPAC layer was unevenly distributed along the length of a channel and between channels in the monolithic membrane.

Keywords: Ceramic microfiltration, Precoating, Super-fine powdered activated carbon, Coagulation

1. Introduction

Pretreatments in low-pressure membrane filtration systems (microfiltration and ultrafiltration) to control hydraulically irreversible membrane fouling, which causes a rapid rise of transmembrane pressure (TMP), have been widely investigated with respect to energy consumption and cost-saving [1–5]. Coagulation is the best available technology among many investigated pretreatments, but coagulation has been inadequate to prevent membrane fouling [6,7] because of its insufficient removal of fouling-causing natural organic matter (NOM), in particular, biopolymers (hydrophilic organic macromolecules with molecular weights [MWs] over 10,000 Da among the NOM) and humic substances (HS) [2,8–10]. A more thorough solution with affordable technology is required to control membrane fouling and reduce operational costs if membrane filtration is to become more popular in water treatment. Integrating coagulation with other accepted pretreatments (e.g., adsorption-coagulation [11,12] and ion exchange–coagulation [13]) has been investigated for multiplier effects, including the mitigation of membrane fouling. Among all combinations, adsorption-coagulation with powdered activated carbon (PAC) has been studied under various circumstances [12,14–16] and widely practiced. The authors of these studies have all reported larger mitigation of membrane fouling with a combination of PAC adsorption and coagulation compared with PAC adsorption alone or coagulation alone. However, PAC is more expensive than coagulant under effective injection rates [17–19], and further increases of efficiency, especially in the case of PAC, are required.

The application of super-fine PAC (SPAC, median diameter 1–2 μm) [20–24] has been considered as a way to meet this requirement. Matsui et al. [25] have reported the

66 superiority of SPAC adsorption-coagulation over conventionally-sized PAC (10-30 μm)
67 adsorption-coagulation in terms of both mitigation of membrane fouling and filtrate water
68 quality. Kanaya et al. [26] have subsequently reported the application of SPAC in a full-
69 scale drinking water treatment plant using ceramic membranes. The SPAC was produced
70 by onsite PAC grinding, and the treatment cost was less than the cost of treatment with
71 PAC. The reduction in the dosage of activated carbon (AC) led to the overall reduction
72 in the treatment cost because the price of AC exceeds the grinding cost.

73 Although the smaller AC particles themselves foul the membrane and cause a greater
74 decline of flux [20–22,27], coagulation pretreatment after AC injection could cancel out
75 this problem [26]. Submicron-sized SPAC (SSPAC, median diameter 200 nm) has
76 recently been shown to successfully retard the hydraulically irreversible membrane
77 fouling of a polymeric membrane [28] because it has a higher capacity to adsorb
78 biopolymers, which are identified as one of the predominant contributors to fouling
79 [10,29,30], than SPAC and conventionally-sized PAC. In addition, unlike the normal
80 dosing operation that involves continuous dosing with SSPAC, dosing with the same
81 amount of SSPAC in a pulse at the beginning of filtration in a submerged polymeric
82 membrane system has been shown to largely retard the rise of membrane pressure [28].
83 This phenomenon has been explained to result from the formation of a precoated layer of
84 the pulse-dosed SSPAC on the membrane, which would prevent foulants from contacting
85 the membrane [28]. However, this previous study has applied SSPAC to only a
86 submerged-type hollow-fiber polymeric (polyvinylidene difluoride [PVDF]) membrane.

87 The application of SSPAC to other types of membranes is of great interest because
88 membranes of many different materials and geometries are used in water treatment.
89 Ceramic membranes have recently been increasingly used because of their superiority

over polymeric membranes in terms of their service lifespan due to their chemical and thermal stability, resistance, and robustness [31–33]. Because of the high cost of ceramic membranes compared with polymeric membranes, mitigating membrane fouling and achieving high-flux filtration are important objectives for lowering capital and operational costs [32]. In addition, SSPAC itself may cause fouling on a ceramic membrane because PAC on a ceramic membrane has been shown to cause cake fouling [34], and the particle size of SSPAC (D10, 0.11 μm; D50, 0.2 μm) is close to the pore size of ceramic membranes (0.1 μm). It is generally understood that the fouling characteristics of ceramic membranes differ from those of polymeric membranes, for example in ways that cause organic fouling to be lower for ceramic membranes than for polymeric membranes [31,32]. It is therefore of great interest to determine how combinations of SSPAC, pulse dose, and ceramic membranes with different geometries affect TMP rise.

This study was conducted with the goal of understanding whether and how pulse dosing of SSPAC attenuates the fouling of ceramic membranes with tubular and monolithic geometries better than continuous dosing with SSPAC. To achieve this goal, experiments were conducted using two very different types of membrane filtration setups that treated diluted secondary-treated municipal wastewater and natural river water through repeated membrane filtrations and hydraulic backwashes. One setup involved a submerged-tubular membrane (hereafter submerged membrane) that enabled vacuum-driven outside-in filtration, whereas the other involved a monolithic membrane that enabled pressure-driven, inside-out filtration.

2. Materials and methods

114

115 *2.1. Waters*

116

117 Two kinds of water were sampled to prepare feedwaters for the membrane filtration
118 experiments. Wanigawa River water (the source of drinking water for the Wanigawa
119 Water Purification Plant, Ibaraki, Japan) was sampled in November of 2020. The water
120 was filtrated through a membrane with a 10-μm pore size (flat-sheet membrane, coated-
121 cellulose-acetate, Y100A142A, Advantec Toyo Kaisha, Ltd., Tokyo, Japan) to prepare
122 feedwater (designated as Water-W-1 and -2) for the experiments with a submerged
123 ceramic membrane system (Section 2.4). The last number in the designation (e.g., 2)
124 indicated the dilution factor.

125

126 Due to the difficulty in obtaining large amount of the river water, another water was
127 prepared by diluting secondary-treated sewage water to simulate contaminated surface
128 water where wastewater flows in. The secondary-treated wastewater was sampled from a
129 sedimentation tank following the activated sludge process at a municipal wastewater
130 treatment plant (Soseigawa Water Reclamation Plaza, Sapporo, Japan) in September and
131 December of 2020 and June of 2021. These waters were filtered through a 10-μm pore
132 size membrane (Y100A142A, Advantec Toyo Kaisha, Ltd.) and diluted with pure water
133 (Milli-Q Advantage, Merck KGaA, Darmstadt, Germany) to prepare the feedwater for
134 experiments with a submerged ceramic membrane or filtered through a 10-μm pore size
135 membrane (a capsule cartridge membrane, polypropylene, CCP-10-E1H, Advantec Toyo
136 Kaisha, Ltd.) and diluted with dechlorinated tap water were used to prepare a large
137 volume of feedwater for experiments with a monolithic ceramic membrane. The

feedwaters prepared from the water sampled in September 2020, December 2020, and June 2021 were designated Water-S-1-4, Water-S-2-4, and Water-S-3-2, respectively. The last number in the designation (e.g., 4) indicated the dilution factor.

Concentrations of dissolved organic carbon (DOC), biopolymers, HS, and ultraviolet absorbance at 260 nm (UV260) were used to characterize the NOM in water. The analytical methods are described in Text 1S of the supplementary information (SI). Table 1S shows the characteristics of the feedwaters.

2.2. Activated carbon and coagulants

SSPAC was prepared by the same procedure previously described [23]. A wood-based, commercially available PAC with a volume median diameter (D50) of 12.7 μm (Taiko-W, Futamura Chemical Co., Ltd., Nagoya, Japan) was dosed into pure water to make a PAC slurry. The PAC slurry was ground in a rotating grinding pot to obtain ACs with D50s of 3.5 μm. The ground AC slurry was then milled in a bead mill to obtain SSPAC with a D50 of 200 nm. The size distribution of the AC particles was measured with an laser diffraction analyzer (Microtrac MT3300EXII, Nikkiso Co., Inc., Tokyo, Japan) after the AC slurries had been supplemented with a dispersant (Triton X-100, Kanto Chemical Co., Tokyo, Japan; final concentration, 0.08% w/v) and then ultra-sonicated [35]. Fig. 2S of the SI shows the size distributions of the AC particles. Poly-aluminum chloride with a basicity of 70% (PACl-70s) and sulfate ion (2% w/w) (Taki Chemical Co., Hyogo, Japan), which is used in actual water treatment plants, was used as the coagulant in this study.

162 *2.3. Ceramic membranes*

163

164 A tubular ceramic membrane for practical use (nominal pore size 0.1 μm, inner
165 diameter 0.9 cm, outer diameter 1.3 cm, length 80 cm, Kubota Corp., Tokyo, Japan) was
166 cut to obtain a piece of membrane with a length of 1.5 cm. One end of the membrane
167 piece was covered with a polyvinyl chloride plate, whereas the other end was covered
168 with a plate with an outlet port, which enabled outside-in filtration by vacuum. The
169 resulting membrane element had a filtration area of 5.3 cm^2 (after considering the
170 adhesion area between the membrane and the plate), which was similar to that of a
171 polymeric membrane (6 cm^2) applied in previous research [28]. All membrane elements
172 were tested for their pure-water permeability and integrity, and membranes with the same
173 permeability were used in the experiments (Fig. 3S, SI).

174 A monolithic ceramic membrane element (nominal pore size 0.1 μm, length 10 cm,
175 diameter 3 cm, channel diameter 1.5 mm, Metawater Co., Tokyo, Japan) was used after
176 sealing some of the membrane channels to reduce the number of channels from 55 to 22
177 or 7 to reduce feedwater consumption in the membrane filtration experiments. Filtration
178 areas were 172 and 54.7 cm^2 for the 22-channel and 7-channel membranes, respectively.
179 Fig. 4S of the SI includes pictures that show the geometries of the membranes.

180

181 *2.4. Submerged ceramic membrane filtration system*

182

183 Panel A of Fig. 1 shows the system setup. The treatment flow except for SSPAC
184 injection was basically the same as that commercialized by Kubota Corp. A rectangular
185 container (2 × 2 × 10 cm height) was used as a submerged-membrane tank, in which a

ceramic membrane element was placed beneath the water. The coagulant was injected in the feed line and mixed with the feedwater by a static mixer to produce a dosage of 2 mg-Al/L, which is the same dosage that was applied in previous experiments with a PVDF membrane [28]. The coagulated water was then fed into the submerged tank after being supplemented with NaOH to bring the pH of the treated water to ~7.5.

In the experiment with the continuous dose of SSPAC, the SSPAC suspension was dosed in the feed line at a dosage of 5 mg/L. In the experiment that involved pulse dosing of SSPAC, the SSPAC was manually dosed in a pulse to the submerged-membrane tank at the beginning of every filtration cycle. This pulse dosing was followed by 30 s of bubbling with an air pump in the tank for mixing. The pulse dosage was equated to the mass of SSPAC calculated from the rate of injection and the concentration of the continuously dosed SSPAC suspension. The overall dosages were therefore the same in the continuous-dosing and pulse-dosing experiments.

Membrane filtration was conducted in an outside-in mode with a flux of 1.93 m/d (80.4 L m^{-2} h^{-1}), which is slightly higher than those applied in actual full-scale plants to clarify membrane fouling in a shorter time but is similar to the previous SSPAC-precoating study [28], unless otherwise noted, using vacuum provided by a peristaltic pump. The membrane was hydraulically backwashed for 30 s every 7 h by pumping pure water in an inside-out direction at a rate of 8.42 m/d (351 L m^{-2} h^{-1}). In additional runs, hydraulic backwashing was conducted by using pure water from a tank under a pressure of 50 or 100 kPa. During the backwash, air-bubbling was conducted in the membrane tank. The water in the submerged-membrane tank was drained after each backwash, and the filtration was then restarted after the tank had filled with feedwater.

The membrane filtrate was collected three times throughout one batch of filtration between backwash cycles. Vacuum pressure was recorded with a pressure meter. The experiments were conducted in a room controlled at a nearly constant temperature of 20 °C, but a digital thermometer was placed in the feedwater tank to monitor the water temperature.

2.5. Monolithic ceramic membrane filtration system

Panel B of Fig. 1 shows the system setup. The treatment flow, except for SSPAC injection, was basically the same as that commercialized by Metawater Co. It consisted of tanks-in-series, including those for coagulation and flocculation, a membrane module, and a hydraulic backwash unit. Two kinds of setups with different configurations were constructed. Setup A was used for a membrane element with 22 channels, whereas Setup B was used for a membrane element with 7 channels.

For Setup A, two treatment lines were set in place and operated in parallel. Feedwater was fed to the first tank, and the coagulant was fed to the fourth tank, where rapid mixing was performed. Slow mixing was performed in the fifth and the sixth tanks, and SSPAC was injected either continuously or in pulses to the sixth tank, from which the water was transferred to the membrane module. In Setup B, coagulant was fed to the fifth tank, where rapid mixing was performed for coagulation. Slow mixing for flocculation was performed in the sixth tank, and SSPAC was injected either continuously to the sixth tank or injected in pulses to the line to the membrane module. The same equipment was used for Setups A and B, but characteristics such as water levels were changed. The pH of the

232 feedwater was adjusted to 7.0 at the beginning, and no other adjustment was conducted
233 during the experiment. The recording data indicated that coagulation pH was 7.5.
234 In both Setups A and B, pulse dosing of SSPAC was performed automatically at
235 predetermined times. To prevent deposition of SSPAC in the injection pipe during the
236 injection shutdown period, the injection pump was operated constantly, and the SSPAC
237 suspension was circulated within a loop of pipe. The pulse injection was therefore not
238 truly a pulse in the strict sense of the word, because it took 5 min to inject a suspension
239 of SSPAC. However, 5 min was much shorter than the times of 2 h (Setup A) and 0.63 h
240 (Setup B) for one batch filtration. It was therefore essentially a pulse injection. Coagulant
241 and SSPAC dosages were 1 mg-Al/L and 2 mg/L, respectively, unless otherwise noted.
242 Table 2S shows other configurations.
243 The membrane filtration was operated in an inside-out mode at a constant flux
244 determined by positive pressure with a periodic hydraulic backwash from the filtrate side
245 at a pressure of 500 kPa unless otherwise noted. The flux was 5 m/d (208 L m^{-2} h^{-1}) for
246 Setup A and 10.5 m/d (438 L m^{-2} h^{-1}) for Setup B: the latter flux was clearly higher than
247 those applied in actual full-scale plants in order to create fouling-prone conditions [6].
248 TMP and water quality were measured in the same way as they were measured in the
249 submerged ceramic membrane filtration system.
250
251 *2.6 Membrane surface observation*
252
253 Photographs of the surface of a tubular membrane were taken with a digital
254 microscope (VHX-2000, Keyence, Osaka, Japan). A rigid industrial fiber microscope
255 (MK012-009-000-45, Olympus, Tokyo, Japan), which reached inside the channels in the

monolithic membrane, was used to take photographs of the surface of the monolithic membrane. The membrane surfaces before filtration, before backwash, and right after backwash were observed.

3. Results

3.1. Changes of TMP in submerged ceramic membrane systems with pulse and continuous dosing of SSPAC

Sixteen runs of membrane filtration were conducted with pulse or continuous dosing of SSPAC using three feedwaters that contained various concentrations of NOM, including biopolymers (Table 1S) that have been thought to cause severe, irreversible membrane fouling [13,30,36].

Runs with continuous dosing of SSPAC were carried out eight times for Water-W-2 (Panel A of Fig. 2), Water-S-2-2, and Water-S-2-4 (Panels B and C of Fig. 2). The TMP rose almost continuously over the duration of the experiment and finally reached ~60 kPa. Among the 8 runs, the TMP rise was not as rapid in only one run (Run 2), but it was still higher than the TMP rise observed in the comparative runs with a pulse dose. The membrane was backwashed every 7 h to clean the membrane and decrease the elevated TMP, but the TMP decreased only marginally after each backwash, and it continued to rise throughout the entire experimental period.

Unlike the runs with continuous dosing of SSPAC, the TMP did not rise as much in the runs that involved pulse dosing of SSPAC. In all eight runs with pulse dosing, the TMP remained low because the backwash worked effectively. Specifically, the increase

280 of the TMP during each 7-h batch filtration was similar to the increase observed during
281 the runs that involved continuous dosing of SSPAC. However, backwashing reduced the
282 TMP to the level that had been observed 7 h earlier, namely at the start of each batch
283 filtration. As a result, pulse dosing was superior to continuous dosing for all runs in terms
284 of attenuating the rise of TMP.

285 The filtration experiments were conducted again for 14 h, and during those
286 experiments the backwash pressure was controlled at 100 kPa or 50 kPa: the use of a
287 pressure tank instead of a peristaltic pump to apply the backwash pressure made it
288 possible to apply a constant backwash pressure more quickly to the membrane. As shown
289 in Fig. 5S of the SI, the TMP increased rapidly probably due to the high DOC of the feed
290 water, and the increase could be reduced only marginally by backwashing if the SSPAC
291 was dosed continuously, but the increase of the TMP was largely reversed by
292 backwashing in the case of pulse dosing of SSPAC.

293

294 *3.2.Changes of TMP in a monolithic ceramic membrane system with pulse and continuous*
295 *dosing of SSPAC*

296

297 The inside-out, pressure-driven monolithic ceramic membrane was tested to compare
298 results with pulse and continuous dosing of SSPAC. In Setup A of the monolithic ceramic
299 membrane, two filtration runs were conducted in parallel; one run employed pulse dosing,
300 and the other run employed continuous dosing. Because the membranes were backwashed
301 every 2 h, the TMP increased for 2 h, decreased because of backwashing, and then
302 increased again. This cycle was repeated, but overall, the TMP gradually increased over
303 the entire time of the system operation. As shown in Panel A of Fig. 3, during the first

five-day operation, the TMP rise was somewhat lower in the system with continuous dosing of SSPAC than in the system with pulse dosing of SSPAC, but the difference of the TMP rise between the two systems was not as large as the difference observed in the submerged ceramic membrane systems (Section 3.1). After five days of operation, each membrane was replaced with a new one, and the two systems were restarted. However, the applications of pulse/continuous dosing to the two systems were inverted (the pulse dosing was applied to Line 1 during days 0–5 and to Line 2 during days 5–9, whereas the continuous dosing was applied to Line 2 during days 0–5 and to Line 1 from days 5–9). After the restart, the TMP rose at a somewhat slower pace in the system with continuous dosing of SSPAC than in the system with pulse dosing, but the difference of the TMP rise between the two systems was again small. Hydraulically reversible rises of TMP (most of the TMP rose in each batch filtration every 2 h was restored by the backwash) were also similar between pulse and continuous dosing (Fig. 6S, SI).

We conducted other runs by using Setup B in which SSPAC was either not dosed, was dosed continuously, or was dosed in pulses directly into the lines to the ceramic membrane. The flux was doubled, and the backwash was repeated more frequently (every 0.63 h) compared with Setup A. The goal of this configuration was to compare pulse and continuous dosing under conditions that were more likely to cause membrane fouling. As shown in Panel B of Fig. 3, the increases of the TMP were lower with pulse and continuous dosing of SSPAC than without SSPAC dosing, but the difference of the TMP rise between the two dosing methods was again small. The superiority of pulse over continuous dosing of SSPAC in attenuating the TMP rise was marginal. The small difference between the two dosing was also observed in the filtration operation with a lower backwash pressure of 50 kPa, which was the same as the backwash pressure applied

328 in the submerged membrane system. TMP rose rapidly due to the low backwash pressure
329 (Fig. 7S, SI), but the rate of TMP buildup was not very different between pulse and
330 continuous SSPAC dosing. Even when the backwash pressure was the same, 50 kPa, the
331 rate of TMP rise was slower in the monolithic membrane system than in the submerged
332 membrane system (Fig. 2), but this difference was caused by the higher backwash
333 frequency in the monolithic membrane system. When the backwash pressure was
334 increased from 50 kPa to 500 kPa during the pulse dose run, the TMP rise was much
335 slower (Fig. 7S, SI).

336 Furthermore, no significant differences in the TMP rise between the systems with
337 pulse and continuous dosing of SSPAC were observed, even when the monolithic
338 membrane system was operated under the same conditions as the submerged membranes
339 (Table 2S). Specifically, we ran the Setup B system at a similar filtration flux of 1.67 m/d
340 (69.8 L m^{-2} h^{-1}), backwash frequency 7 h, pressure of 50 kPa, coagulant dosage 2 mg-
341 Al/L, and SSPAC dosage of 5 mg/L. The changes of TMP were almost the same for pulse
342 and continuous dosing of SSPAC (Fig. 8S, SI).

343

344 *3.3. Filtrate qualities between pulse and continuous dosing of SSPAC in submerged and*
345 *monolithic ceramic membrane systems*

346

347 Feedwater and filtrate were sampled in the membrane filtration experiments, and the
348 DOC and UV260 were assessed to evaluate water quality. For the submerged ceramic
349 membrane filtration system, continuous dosing of SSPAC achieved DOC removals of
350 10–20% and UV260 removal of 30–40%, whereas pulse dosing of SSPAC achieved 40–
351 50% removal of DOC and 60–70% removal of UV260 (Fig. 4). The difference in the

352 removal percentages of these two dosing methods was observed for all three feedwaters
353 tested. Pulse dosing of SSPAC removed HS more than continuous dosing of SSPAC. The
354 superiority of pulse dosing was not observed for biopolymers because biopolymers were
355 almost completely removed by both pulse and continuous dosing of SSPAC.
356 In the case of the monolithic ceramic membrane system, continuous dosing of SSPAC
357 resulted in slightly higher removals of DOC and HS from Water-S-2-2 but not from Water
358 S-1-4 (Fig. 5). Removal rates of DOC and E260 were overall 40–50%, no matter what
359 dosing methods were used. The removal of biopolymer slightly exceeded 60%. Except
360 for the concentrations of DOC and HS in Water-S-2-2, pulse and continuous dosing of
361 SSPAC did not appear to result in significant differences in the qualities of filtrates based
362 on DOC (including biopolymers and HS) and UV260.
363
364 *3.4. Surface observations of submerged and monolithic ceramic membranes*
365
366 The surfaces of submerged membranes were observed by taking photographs (Panels
367 A-D in Fig. 6 and Fig. 9S of the SI). The surface of the membrane was initially white, but
368 after 30 min, which was the hydraulic retention time of the submerged membrane tank,
369 part of the membrane surface remained white, but most of it had turned black. The black
370 area was larger in the pulse dosing than in the continuous dosing of SSPAC. After a 7-h
371 filtration, the membrane surface appeared to be covered with a layer of suspended solids,
372 including SSPAC. After backwashing, the surface of the membrane was white with many
373 black spots in the case of pulse dosing. In the case of continuous dosing, the black layer
374 remained and covered most of the membrane.
375

376 The surfaces of a monolithic membrane were observed with a fiber microscope, which
377 was inserted into the membrane channels. The photographs (Observation 1) were first
378 taken in the middle part of a channel of a blank membrane, a membrane after a 5-min
379 filtration, a membrane after a 0.63-h filtration, and a membrane immediately after
380 backwashing (Panels A–D in Fig. 10S of the SI, respectively). The inside of the
381 membrane channel (middle part of channel no. 1 in Fig. 11S, SI) became black 5 min
382 after a pulse dose of SSPAC, but it did not after a continuous dose of SSPAC. After
383 filtration for 0.63 h, which took place immediately before backwashing, the channels of
384 the membrane had become black for both systems with a pulse and a continuous dose of
385 SSPAC. Their color returned to white after backwashing, but a few black particles were
386 observed for the system with a continuous dose but not the system with a pulse dose.
387 To further understand the accumulation of SSPAC in channels after a pulse dose of
388 SSPAC, we observed all the channels of a membrane element after a 5-min filtration run.
389 The SSPAC dosage was increased from 2 mg/L to 5 mg/L to observe the accumulation
390 of SSPAC more clearly, and the experiments were conducted six times. In Fig. 7
391 (Observation 2), we observed that the no. 1 channel, which was located in the middle of
392 the membrane, was blacker than the other channels. The indication was that the
393 distribution of SSPAC was uneven between channels. In Observation 3 (Fig. 12S, SI),
394 which involved the same membrane element as Observation 2, the black area seemed to
395 have become more even than in Observation 2, but a non-uniformity of the black area
396 between channels was still observed at the inlet (lower part) of channels 2, 4, 5, and 6.
397 Such non-uniformity was also apparent in some channels during Observation 2 (Fig. 7).
398 The uneven distribution of SSPAC particles between channels and the non-uniformity of

399 the black area in a channel were also observed in Observations 4 and 5 (Figs. 13S-14S,
400 SI), where the membrane elements differed from those used in Observations 2 and 3.
401 Based on the above results, observation experiments to compare a pulse and a
402 continuous dose were conducted again, but floc particles that had grown large were
403 present in the slow mixing tank (Observations 6 and 7). As shown in Fig. 8 and Fig. 15S
404 of the SI, black particles were found mostly in the lower part of the channels and were
405 distributed unevenly. They were seldom observed in the middle and upper parts of
406 channels.
407
408 **4. Discussion**
409
410 *4.1 Effectiveness of pulse dosing of SSPAC for mitigating hydraulically irreversible*
411 *membrane fouling*
412
413 A previous study [28] has recently shown that pulse dosing of SSPAC to a submerged
414 polymeric membrane filtration system can suppress the increase of TMP during filtration
415 better than continuous dosing of SSPAC. However, this result was obtained with one type
416 of polymeric membrane system: an outside-in, vacuum-driven, submerged type. In this
417 study, the pulse dosing of SSPAC was shown to be effective for the ceramic inorganic
418 membrane of an outside-in, vacuum-driven, submerged membrane, but it was not
419 effective for an inside-out, pressure-driven, monolithic membrane. As described in
420 Section 3.1, when SSPAC was dosed in pulses in the tank where the membrane had been
421 submerged after the membrane was backwashed, the TMP did not increase (Text 2S and
422 Table 4S, SI).

423 The attenuation of TMP buildup by the pulse-dosed SSPAC can be explained by 1)
424 higher adsorption capacity of SSPAC than SPAC and PAC on NOM especially for
425 biopolymers [28], which is regarded as the dominant contributor to irreversible fouling
426 [29,37–39]; and 2) formation of a precoat SSPAC layer on the membrane surface in the
427 initial stage of every batch filtration by a pulse dose of SSPAC. In this study, we
428 conducted the adsorption isotherm experiments by using PAC, SPAC, and SSPAC. As
429 shown in Fig. 16S of the SI, SSPAC adsorbed foulants (especially biopolymers) better
430 than PAC and SPAC at low dosages. The precoat SSPAC effectively removes NOM, in
431 particular biopolymer, by straining (mechanical separation) as well as by adsorption. In
432 our previous study [28], the straining effect of the SSPAC precoat layer is investigated
433 by using an analytical MCE (mixed cellulose esters) flat-sheet membrane. In the present
434 study, we conducted a batch experiment by using precoat layer of non-adsorbent,
435 submicron polystyrene latex (PSL) particles (particle diameter; 200 nm) on top of a flat
436 sheet ceramic membrane (Table 3S, SI). The results shown in Fig. 17S of the SI indicate
437 that the precoat layer composed of submicron particles strains a portion of biopolymers
438 out. On the surface of the ceramic membrane submerged in water, the formation of the
439 precoat layer was actually observed (Section 3.4). Therefore, mechanism 2) as well as
440 mechanism 1) are applicable to the submerged ceramic membrane with vacuum-driven,
441 outside-in filtration. Better removal by pulse dosing of SSPAC than continuous dosing of
442 SSPAC was actually observed for HS. We had expected higher biopolymer removal by
443 pulse dosing of SSPAC. In fact, the rate of biopolymer removal by pulse-dosed SSPAC
444 was high, as described in Section 3.3. However, the biopolymer removal by continuously
445 dosed SSPAC was also high probably due to high dose of SSPAC and/or coagulant, so
446 the difference in biopolymer removal between the two dosing methods was unclear. The

high removal of NOM in conjunction with the membrane surface observations (Section 3.4) suggests that pulse dosing of SSPAC can form a better precoat layer than continuous dosing of SSPAC and the precoat layer of SSPAC removed HS as well as biopolymers and resulted in the high mitigation of membrane fouling.

In contrast, it is likely that SSPAC itself causes membrane fouling because activated carbon tends to adhere firmly to the surface of ceramic membranes [34]. Moreover, the particle size of SSPAC (D10, 0.11 μm; D50, 0.2 μm) is close to the pore size of ceramic membranes (nominal size of 0.1 μm). Therefore, it is very likely that SSPAC itself is a strong membrane foulant. However, as described in Section 3.4, the SSPAC on the surface of the membrane was cleared after a backwash because of coagulation pretreatment. This is in accordance with the fact that ceramic membrane filtration is often operated with coagulation pretreatment [40–42]. Fouling of ceramic membranes by particulate matter is likely to occur without coagulation pretreatment. Moreover, the SSPAC was cleared at a lesser extent when the SSPAC was dosed in a continuous than when the SSPAC was dosed in a pulse. This difference is related to the difference in the TMP increase between pulse and continuous dosing.

4.2 Importance of precoat layer formation

In the inside-out monolithic ceramic membrane system, pulse dosing of SSPAC did not appear markedly superior to continuous dosing of SSPAC: the increases of the TMP were similar (Section 3.2). In the case of filtrate quality such as DOC, there was no consistent trend: neither pulse nor continuous dosing was consistently better, as described

471 in Section 3.3. In other words, the effectiveness of the pulse dosing of SSPAC differed
472 for the two ceramic membranes: the monolithic ceramic membrane and the submerged
473 ceramic membrane. The nominal pore sizes of the two ceramic membranes are the same
474 (Table 3S), but the structure of the membranes is very different (inside-out monolithic vs.
475 outside-in tubular).

476 Another major difference between the two ceramic membrane systems is the
477 operating pressure. Monolithic ceramic membrane systems are usually operated at a high
478 flux because the filtration was pressurized, and the pressure during backwashing is also
479 high [31,43]. In contrast, submerged ceramic membranes are filtered by suction pressure,
480 so the available TMP is smaller than in the case of monolithic ceramic membrane systems
481 [44,45]. In most of the experiments, we applied a higher filtration flux with a higher
482 backwash pressure to the monolithic membrane than to the submerged membrane. This
483 operation is in accordance with the practice of full-scale, drinking water treatment plants.
484 However, when the backwash pressure in the submerged membrane was doubled and was
485 applied from a pressure tank (as it was in the monolithic system), the superiority of the
486 pulse dosing of SSPAC over the continuous dosing of SSPAC dose was maintained, as
487 described in Section 3.1. In contrast, even when the filtration flux and backwash pressure
488 in the monolithic membrane were decreased to the same levels as in the submerged
489 membrane, the performances of the pulse dosing of SSPAC and the continuous dosing of
490 SSPAC were still the same, as described in Section 3.2. The differences in the
491 effectiveness of the pulse dosing of SSPAC on the two ceramic membranes were thus
492 unrelated to the backwash pressure and its method of application.

493 In addition, the TMP was much lower in the monolithic membrane than in the submerged
494 membrane, even when the backwash interval, filtration flux, and chemical dosages were

the same in the two systems. The implication is that the coagulation-flocculation process in the mixing tanks of the monolithic membrane system achieved better performance than the static mixer in the submerged ceramic membrane system. Although it is recognized that further research is needed to determine the optimum mixing conditions for SSPAC pre-coating, this study was not able to go that far.

Coagulation plays an important role in preventing membrane fouling due to SSPAC particles themselves [28]. On the other hand, it is reported that synergetic fouling exists between PAC and organic foulants such as humic acid [46]. Biopolymers are well removed by the precoating of SSPAC, but the TMP during the filtration becomes high without coagulation pretreatment [22]. Our previous study also revealed that when SSPAC is pulse-dosed to form precoating without coagulation pretreatment, the rise of TMP was canceled only partially by hydraulic backwash, indicating that SSPAC itself contributes to irreversible fouling [28]. However, when the coagulant was added before filtration, the effectiveness of the hydraulic backwash was remarkably enhanced. It can be explained such that the coagulant loosens the bonding between the membrane and SSPAC layer, and thus the irreversible fouling due to SSPAC is prevented [28]. Further elucidation of the phenomenon requires experimental analysis, such as quantifying the organic foulants at different depths of the SSPAC layer. In order to conduct such a study, however, further challenges would be necessary for not only slice sampling but also the separation of activated carbon and organic foulant [47,48].

The important difference between the two ceramic membranes was the formation of the precoat layer on the membrane surface. In the submerged membrane system, we observed that the membrane surface became black with SSPAC at a higher rate when SSPAC was applied in a pulse dose than a continuous dose (Section 3.4). This result

519 indicates that the formation of a precoat layer of SSPAC is rapid in the case of pulse
520 dosing compared to continuous dosing. Moreover, the SSPAC precoat layer was cleared
521 by the backwash more efficiently. In contrast, in the monolithic membrane system, we
522 observed the accumulation of SSPAC, but it was unevenly distributed. Some channels
523 were loaded more with SSPAC than other channels (Section 3.4). Heijman et al. [22] have
524 mentioned the possibility of an uneven distribution of precoated SPAC, but they do not
525 include any data relevant to this possibility. In this study, we observed an uneven
526 distribution of pulse-dosed SSPAC, which we had expected to form a uniform precoat.
527 The non-uniform distribution was clearly apparent when large floc particles along with
528 SSPAC were introduced into the membrane.

529 Moreover, the degree of non-uniformity of the distribution differed somewhat
530 between the two filtration experiments (Observations 2 and 3 in Section 3.4), although
531 the same membrane element was used. This difference suggests that the non-uniform
532 coating was caused not only by the effects of non-uniform flow distribution at the inlet of
533 an element and any differences in factors such as local permeability but also by stochastic
534 factors. In a full-scale membrane element, there are 2000 channels in one membrane
535 element, and the length of the membrane is much longer: it is 1.5 m. Therefore, it would
536 be more difficult to suppress the non-uniformity of the distribution of the pulse-dosed
537 SSPAC and to precoat the membrane surface evenly with SSPAC in a full-scale plant
538 than in a laboratory experimental setup like this study.

539 In the case of a submerged membranes system, when the scale of the system reaches
540 full scale with many tubes of membranes elements, it is also necessary to provide a
541 method to uniformly precoat all the membrane tubes with pulse-dosed SSPAC. The tank
542 of a full-scale, submerged ceramic membrane filtration system is aerated with bubbles to

543 reduce membrane fouling, but this aeration of the tank may also be effective in forming
544 a uniform precoating. We cut tubular ceramic membranes 0.8 m in length to make small
545 membrane elements for the experiment in this study, but we observed that the pure-water
546 permeabilities of the small membrane elements differed (Fig. 3S, SI). These differences
547 indicated that the permeabilities of the membrane elements varied locally from place to
548 place along the tube length. The filtration rate, namely the precoating rate, was therefore
549 affected not only by local variation in hydraulic conditions but also by local variations of
550 membrane permeability. This study enabled us to consider the possibility that there were
551 local differences in the permeation rate of the membrane, and those differences may have
552 affected the success or failure of the precoating method. This possibility is important to
553 consider when apply pulse dosing of SSPAC to a full-scale membrane filtration system.
554
555 **5. Conclusions**
556
557 Pulse and continuous dosing of SSPAC, which can efficiently remove NOM because
558 of its high adsorption capacity, were applied as pretreatments for two different types of
559 ceramic membrane filters (an outside-in vacuum-driven submerged membrane and an
560 inside-out pressure-driven monolithic membrane) to try to attenuate increases of TMP
561 due to the irreversible membrane fouling during filtration with periodic hydraulic
562 backwashing. Major findings of the study were as follows:
563
564 (1) Pulse dosing of SSPAC prevented TMP rise more than continuous dosing of SSPAC
565 in the submerged membrane filtration system with a ceramic membrane. A precoating
566 layer composed of SSPAC formed evenly on the ceramic membrane surface and was

567 peeled off cleanly by hydraulic backwashing in the case of the pulse dosing of SSPAC.
568 High removal of NOM (including biopolymer and HS) and a uniform layer of SSPAC,
569 which prevented attachment of NOM to the membrane surface at the beginning of
570 filtration, was thought to be the cause.
571
572 (2) In monolithic ceramic membrane systems, pulse dosing of SSPAC did not alleviate
573 TMP rise better than continuous dosing of SSPAC and did not remove NOM better. The
574 uneven distribution of pulse-dosed SSPAC in the membrane channels was thought to be
575 a cause of the lack of any difference between the efficacy of the pulse dosing of SSPAC
576 over the continuous dosing. The higher backwash pressure in the monolithic ceramic
577 membrane system versus the submerged membrane filtration was not the cause of the
578 absence of a treatment effect.
579
580 **Acknowledgments**
581
582 This work was supported by supported by a JSPS Grant-in-Aid for Scientific Research
583 S (no. 16H06362) and A (no. 21H04567) and by JST SPRING (no. JPMJSP2119). The
584 authors gratefully acknowledge Futamura Chemical for providing PAC samples; Taki
585 Chemical for coagulants; Kubota Corp. and Metawater Co. for membranes; Ibaraki
586 Prefectural Waterworks Bureau and Sewerage & Rivers Bureau of Sapporo City for water
587 samplings.
588
589 **References**
590

591 [1] W. Gao, H. Liang, J. Ma, M. Han, Z. lin Chen, Z. shuang Han, G. bai Li, Membrane
592 fouling control in ultrafiltration technology for drinking water production: A review,
593 Desalination. 272 (2011) 1–8. https://doi.org/10.1016/j.desal.2011.01.051.
594 [2] D.T. Myat, M. Mergen, O. Zhao, M.B. Stewart, J.D. Orbell, T. Merle, J.P. Croué, S.R.
595 Gray, Membrane fouling mechanism transition in relation to feed water composition, J.
596 Memb. Sci. 471 (2014) 265–273. https://doi.org/10.1016/j.memsci.2014.07.067.
597 [3] S. Azizighannad, W. Intrchom, S. Mitra, Raman imaging of membrane fouling, Sep.
598 Purif. Technol. 242 (2020) 116763. https://doi.org/10.1016/j.seppur.2020.116763.
599 [4] J. Lohwacharin, K. Oguma, S. Takizawa, Use of carbon black nanoparticles to mitigate
600 membrane fouling in ultrafiltration of river water, Sep. Purif. Technol. 72 (2010) 61–69.
601 https://doi.org/10.1016/j.seppur.2010.01.003.
602 [5] Y. Zhang, Q. Fu, Algal fouling of microfiltration and ultrafiltration membranes and
603 control strategies: A review, Sep. Purif. Technol. 203 (2018) 193–208.
604 https://doi.org/10.1016/j.seppur.2018.04.040.
605 [6] M. Kimura, Y. Matsui, S. Saito, T. Takahashi, M. Nakagawa, N. Shirasaki, T.
606 Matsushita, Hydraulically irreversible membrane fouling during coagulation-
607 microfiltration and its control by using high-basicity polyaluminum chloride, J. Memb.
608 Sci. 477 (2015) 115–122. https://doi.org/10.1016/j.memsci.2014.12.033.

609 [7] S. Wang, C. Liu, Q. Li, Impact of polymer flocculants on coagulation-microfiltration of
610 surface water, Water Res. 47 (2013) 4538–4546.
611 https://doi.org/10.1016/j.watres.2013.04.040.
612 [8] Q. Ding, H. Yamamura, H. Yonekawa, N. Aoki, N. Murata, A. Hafuka, Y. Watanabe,
613 Differences in behaviour of three biopolymer constituents in coagulation with
614 polyaluminium chloride: Implications for the optimisation of a coagulation–membrane
615 filtration process, Water Res. 133 (2018) 255–263.
616 https://doi.org/10.1016/j.watres.2018.01.034.
617 [9] V.L. Quang, I. Choi, J. Hur, Tracking the behavior of different size fractions of dissolved
618 organic matter in a full-scale advanced drinking water treatment plant, Environ. Sci.
619 Pollut. Res. 22 (2015) 18176–18184. https://doi.org/10.1007/s11356-015-5040-3.
620 [10] K. Kimura, K. Shikato, Y. Oki, K. Kume, S.A. Huber, Surface water biopolymer
621 fractionation for fouling mitigation in low-pressure membranes, J. Memb. Sci. (2018)
622 554, 83–89. https://doi.org/10.1016/j.memsci.2018.02.024.
623 [11] R. Fabris, E.K. Lee, C.W.K. Chow, V. Chen, M. Drikas, Pre-treatments to reduce
624 fouling of low pressure micro-filtration (MF) membranes, J. Memb. Sci. 289 (2007)
625 231–240. https://doi.org/10.1016/j.memsci.2006.12.003.

626 [12] W. Yu, L. Xu, J. Qu, N. Graham, Investigation of pre-coagulation and powder activate
627 carbon adsorption on ultrafiltration membrane fouling, J. Memb. Sci. 459 (2014) 157–
628 168. https://doi.org/10.1016/j.memsci.2014.02.005.
629 [13] K. Kimura, Y. Oki, Efficient control of membrane fouling in MF by removal of
630 biopolymers: Comparison of various pretreatments, Water Res. 115 (2017) 172–179.
631 https://doi.org/10.1016/j.watres.2017.02.033.
632 [14] C. Schwaller, G. Hoffmann, C.X. Hiller, B. Helmreich, J.E. Drewes, Inline dosing of
633 powdered activated carbon and coagulant prior to ultrafiltration at pilot-scale – Effects
634 on trace organic chemical removal and operational stability, Chem. Eng. J. 414 (2021).
635 https://doi.org/10.1016/j.cej.2021.128801.
636 [15] H. Wang, F. Qu, A. Ding, H. Liang, R. Jia, K. Li, L. Bai, H. Chang, G. Li, Combined
637 effects of PAC adsorption and in situ chlorination on membrane fouling in a pilot-scale
638 coagulation and ultrafiltration process, Chem. Eng. J. 283 (2016) 1374–1383.
639 https://doi.org/10.1016/j.cej.2015.08.093.
640 [16] J. Xing, H. Liang, X. Cheng, H. Yang, D. Xu, Z. Gan, X. Luo, X. Zhu, G. Li, Combined
641 effects of coagulation and adsorption on ultrafiltration membrane fouling control and
642 subsequent disinfection in drinking water treatment, Environ. Sci. Pollut. Res. 26 (2019)
643 33770–33780. https://doi.org/10.1007/s11356-018-2416-1.

644 [17] J. Mallevialle, P.E. Odendaal, M.R. Wiesner, Water treatment membrane processes,
645 American Water Works Association, 1996.
646 [18] A. Khazaie, M. Mazarji, B. Samali, D. Osborne, T. Minkina, S. Sushkova, S.
647 Mandzhieva, A. Soldatov, A Review on Coagulation / Flocculation in Dewatering of
648 Coal Slurry, Water. 14(6) (2022) 918. https://doi.org/10.3390/w14060918.
649 [19] E. Menya, P.W. Olupot, H. Storz, M. Lubwama, Y. Kiros, Production and performance
650 of activated carbon from rice husks for removal of natural organic matter from water: A
651 review, Chem. Eng. Res. Des. 129 (2018) 271–296.
652 https://doi.org/10.1016/j.cherd.2017.11.008.
653 [20] N. Ando, Y. Matsui, R. Kurotobi, Y. Nakano, T. Matsushita, K. Ohno, Comparison of
654 natural organic matter adsorption capacities of super-powdered activated carbon and
655 powdered activated Carbon, Water Res. 44 (2010) 4127–4136.
656 https://doi.org/10.1016/j.watres.2010.05.029.
657 [21] Y. Matsui, T. Sanogawa, N. Aoki, S. Mima, T. Matsushita, Evaluating submicron-sized
658 activated carbon adsorption for microfiltration pretreatment, Water Sci. Technol. Water
659 Supply. 6 (2006) 149–155. https://doi.org/10.2166/ws.2006.017.

660 [22] S.G.J. Heijman, J.Z. Hamad, J. Schippers, G. Amy, M.D. Kennedy, Submicron
661 powdered activated carbon used as a pre-coat in ceramic micro-filtration, Desalin. Water
662 Treat. 9 (2009) 86–91. https://doi.org/10.5004/dwt.2009.755.
663 [23] L. Pan, Y. Nishimura, H. Takaesu, Y. Matsui, T. Matsushita, N. Shirasaki, Effects of
664 decreasing activated carbon particle diameter from 30 Mm to 140 nm on equilibrium
665 adsorption capacity, Water Res. 124 (2017) 425–434.
666 https://doi.org/10.1016/j.watres.2017.07.075.
667 [24] J.R. Ellerie, O.G. Apul, T. Karanfil, D.A. Ladner, Comparing graphene, carbon
668 nanotubes, and superfine powdered activated carbon as adsorptive coating materials for
669 microfiltration membranes, J. Hazard. Mater. 261 (2013) 91–98.
670 https://doi.org/10.1016/j.jhazmat.2013.07.009.
671 [25] Y. Matsui, H. Hasegawa, K. Ohno, T. Matsushita, S. Mima, Y. Kawase, T. Aizawa,
672 Effects of super-powdered activated carbon pretreatment on coagulation and trans-
673 membrane pressure buildup during microfiltration, Water Res. 43 (2009) 5160–5170.
674 https://doi.org/10.1016/j.watres.2009.08.021.
675 [26] S. Kanaya, Y. Kawase, S. Mima, K. Sugiura, K. Murase, H. Yonekawa, Drinking water
676 treatment using superfine PAC (SPAC): Design and successful operation history in full-
677 scale plant, Am. Water Work. Assoc. Salt Lake City, Utah, USA, Pp. (2015) 624–631.

678 [27] E. Partlan, Superfine Powdered Activated Carbon (S-PAC) Coupled with
679 Microfiltration for the Removal of Trace Organics in Drinking Water Treatment,
680 Doctoral dissertations, Clemson University, 2017.
681 [28] Y. Zhao, R. Kitajima, N. Shirasaki, Y. Matsui, T. Matsushita, Precoating membranes
682 with submicron super-fine powdered activated carbon after coagulation prevents
683 transmembrane pressure rise: Straining and high adsorption capacity effects, Water Res.
684 177 (2020) 115757. https://doi.org/10.1016/j.watres.2020.115757.
685 [29] J. Tian, M. Ernst, F. Cui, M. Jekel, Correlations of relevant membrane foulants with UF
686 membrane fouling in different waters., Water Res. 47 (2013) 1218–28.
687 https://doi.org/10.1016/j.watres.2012.11.043.
688 [30] S.A. Huber, A. Balz, M. Abert, W. Pronk, Characterisation of aquatic humic and non-
689 humic matter with size-exclusion chromatography - organic carbon detection - organic
690 nitrogen detection (LC-OCD-OND), Water Res. 45 (2011) 879–885.
691 https://doi.org/10.1016/j.watres.2010.09.023.
692 [31] M.B. Asif, Z. Zhang, Ceramic membrane technology for water and wastewater
693 treatment: A critical review of performance, full-scale applications, membrane fouling
694 and prospects, Chem. Eng. J. 418 (2021) 129481.
695 https://doi.org/10.1016/j.cej.2021.129481.

[32] S.M. Samaei, S. Gato-Trinidad, A. Altaee, The application of pressure-driven ceramic membrane technology for the treatment of industrial wastewaters – A review, Sep. Purif. Technol. 200 (2018) 198–220. https://doi.org/10.1016/j.seppur.2018.02.041.

[33] A. Murić, I. Petrinić, M.L. Christensen, Comparison of ceramic and polymeric ultrafiltration membranes for treating wastewater from metalworking industry, Chem. Eng. J. 255 (2014) 403–410. https://doi.org/10.1016/j.cej.2014.06.009.

[34] P. Zhao, S. Takizawa, H. Katayama, S. Ohgaki, Factors causing PAC cake fouling in PAC-MF (powdered activated carbon-microfiltration) water treatment systems, Water Sci. Technol. 51 (2005) 231–240. https://doi.org/10.2166/wst.2005.0642.

[35] L. Pan, Y. Matsui, T. Matsushita, N. Shirasaki, Superiority of wet-milled over dry-milled superfine powdered activated carbon for adsorptive 2-methylisoborneol removal, Water Res. 102 (2016) 516–523. https://doi.org/10.1016/j.watres.2016.06.062.

[36] F. Chen, S. Peldszus, R.H. Peiris, A.S. Ruhl, R. Mehrez, M. Jekel, R.L. Legge, P.M. Huck, Pilot-scale investigation of drinking water ultrafiltration membrane fouling rates using advanced data analysis techniques, Water Res. 48 (2014) 508–518. https://doi.org/10.1016/j.watres.2013.10.007.

[37] C. Ayache, M. Pidou, J.P. Croué, J. Labanowski, Y. Poussade, A. Tazi-Pain, J. Keller, W. Gernjak, Impact of effluent organic matter on low-pressure membrane fouling in

714 tertiary treatment, Water Res. 47 (2013) 2633–2642.
715 https://doi.org/10.1016/j.watres.2013.01.043.
716 [38] B.C. Huang, Y.F. Guan, W. Chen, H.Q. Yu, Membrane fouling characteristics and
717 mitigation in a coagulation-assisted microfiltration process for municipal wastewater
718 pretreatment, Water Res. 123 (2017) 216–223.
719 https://doi.org/10.1016/j.watres.2017.06.080.
720 [39] K. Kimura, K. Tanaka, Y. Watanabe, Microfiltration of different surface waters
721 with/without coagulation: Clear correlations between membrane fouling and hydrophilic
722 biopolymers, Water Res. 49 (2014) 434–443.
723 https://doi.org/10.1016/j.watres.2013.10.030.
724 [40] S.-J. Lee, J.-H. Kim, Effects of coagulation on the ceramic membrane fouling during
725 surface water treatment, J. Environ. Eng. 141 (2015) 4014087.
726 https://doi.org/https://doi.org/10.1061/(ASCE)EE.1943-7870.0000918.
727 [41] H. Zhu, X. Wen, X. Huang, Characterization of membrane fouling in a microfiltration
728 ceramic membrane system treating secondary effluent, Desalination. 284 (2012) 324–
729 331. https://doi.org/10.1016/j.desal.2011.09.019.

730 [42] A. Alansari, M. Selbes, T. Karanfil, J. Amburgey, Optimization of coagulation
731 pretreatment conditions in a ceramic membrane system, J. Am. Water Works Assoc. 107
732 (2015) E693–E701. https://doi.org/10.5942/jawwa.2015.107.0151.
733 [43] City of Yokohama, Kawai Purification Plant, Kanagawa, Japan, (2018).
734 https://www.city.yokohama.lg.jp/kurashi/sumai-kurashi/suido-
735 gesui/suido/suishitsu/josuijo/kawai/gaiyou.html (accessed February 1, 2022).
736 [44] S. Dong, E.S. Kim, A. Alpatova, H. Noguchi, Y. Liu, M. Gamal El-Din, Treatment of oil
737 sands process-affected water by submerged ceramic membrane microfiltration system,
738 Sep. Purif. Technol. 138 (2014) 198–209. https://doi.org/10.1016/j.seppur.2014.10.017.
739 [45] Nagahoro Water Supply Authority, The First Water Treatment Plant, Hokkaido, Japan,
740 (2006). http://www.nagahoro.jp/authority/plant_01/ (accessed February 1, 2022).
741 [46] S. Shao, H. Liang, F. Qu, K. Li, H. Chang, H. Yu, G. Li, Combined influence by humic
742 acid (HA) and powdered activated carbon (PAC) particles on ultrafiltration membrane
743 fouling, J. Memb. Sci. 500 (2016) 99–105.
744 https://doi.org/10.1016/j.memsci.2015.11.036.
745 [47] G. Aschermann, L. Neubert, F. Zietzschmann, M. Jekel, Impact of different DOM size
746 fractions on the desorption of organic micropollutants from activated carbon, Water Res.
747 161 (2019) 161–170. https://doi.org/10.1016/j.watres.2019.05.039.

748 [48] C. Pelekani, V.L. Snoeyink, Competitive adsorption in natural water: Role of activated
749 carbon pore size, Water Res. 33 (1999) 1209–1219. https://doi.org/10.1016/S0043-
750 1354(98)00329-7.
751 [49] P. Kovalsky, X. Wang, G. Bushell, T.D. Waite, Application of local material properties
752 to prediction of constant flux filtration behaviour of compressible matter ℭ, 318 (2008)
753 191–200. https://doi.org/10.1016/j.memsci.2008.02.044.
754

Research highlights:

1. Submicron super-fine powdered activated carbon prevents transmembrane pressure rise.

2. Pulse dosing is superior to continuous dosing for submerged ceramic membranes.

3. Pulse and continuous dosing have similar effects in a monolithic ceramic membrane.

4. Uniform precoat layer was formed on the submerged but not the monolithic membrane.

5. Precoat layer was peeled off cleanly by hydraulic backwash.

Submerged membrane
(outside-in filtration)

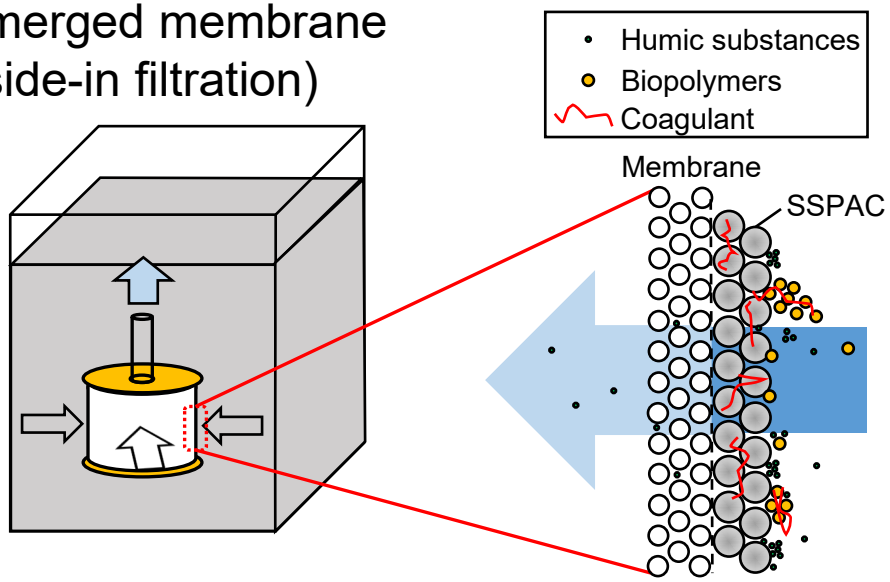

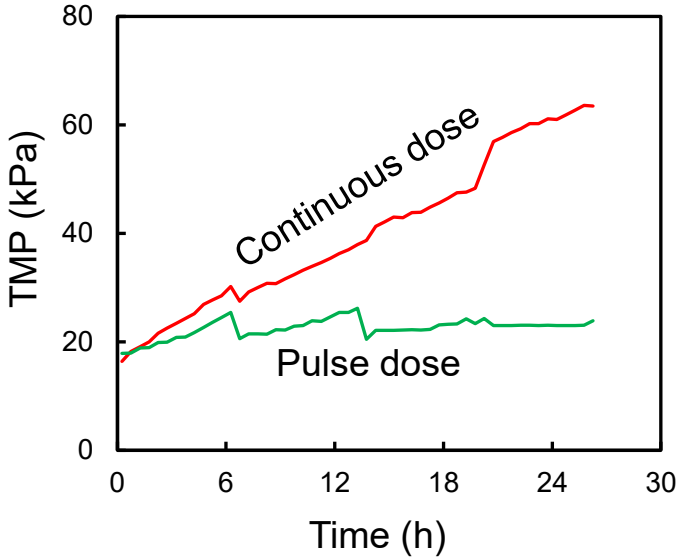

Monolithic membrane
(inside-out filtration)

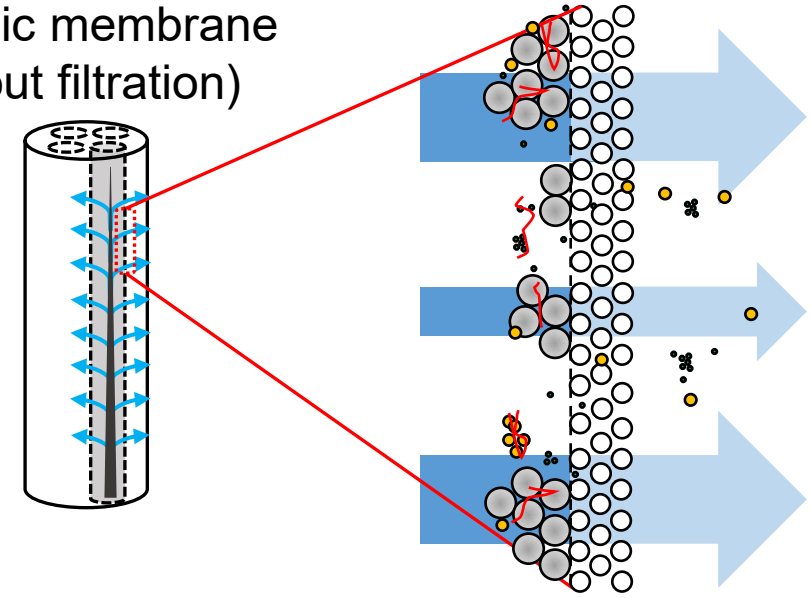

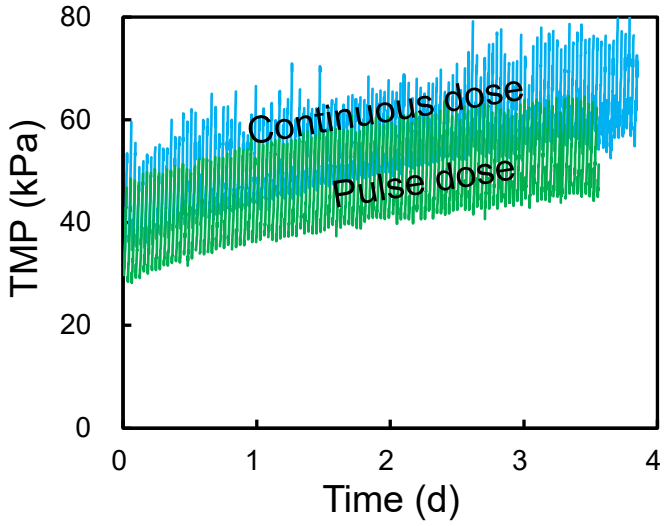

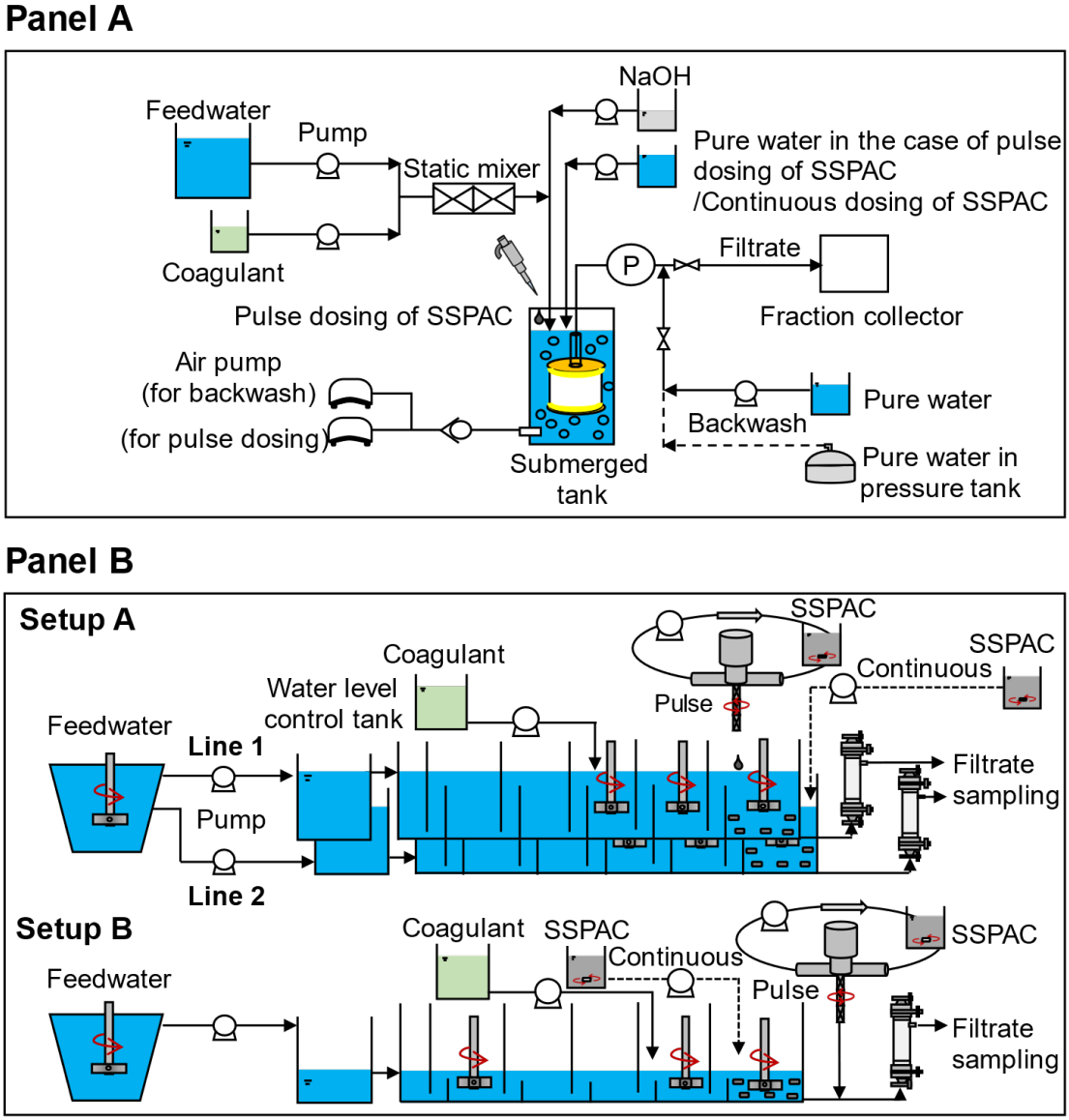

Fig. 1. System setups for submerged membrane (Panel A) and monolithic membrane (Panel B) with pulse and continuous dosing with submicron super-fine powdered activated carbon (SSPAC). Setup A of the monolithic membrane had two treatment lines with the same configuration and were operated in parallel, whereas Setup B had a single treatment line.

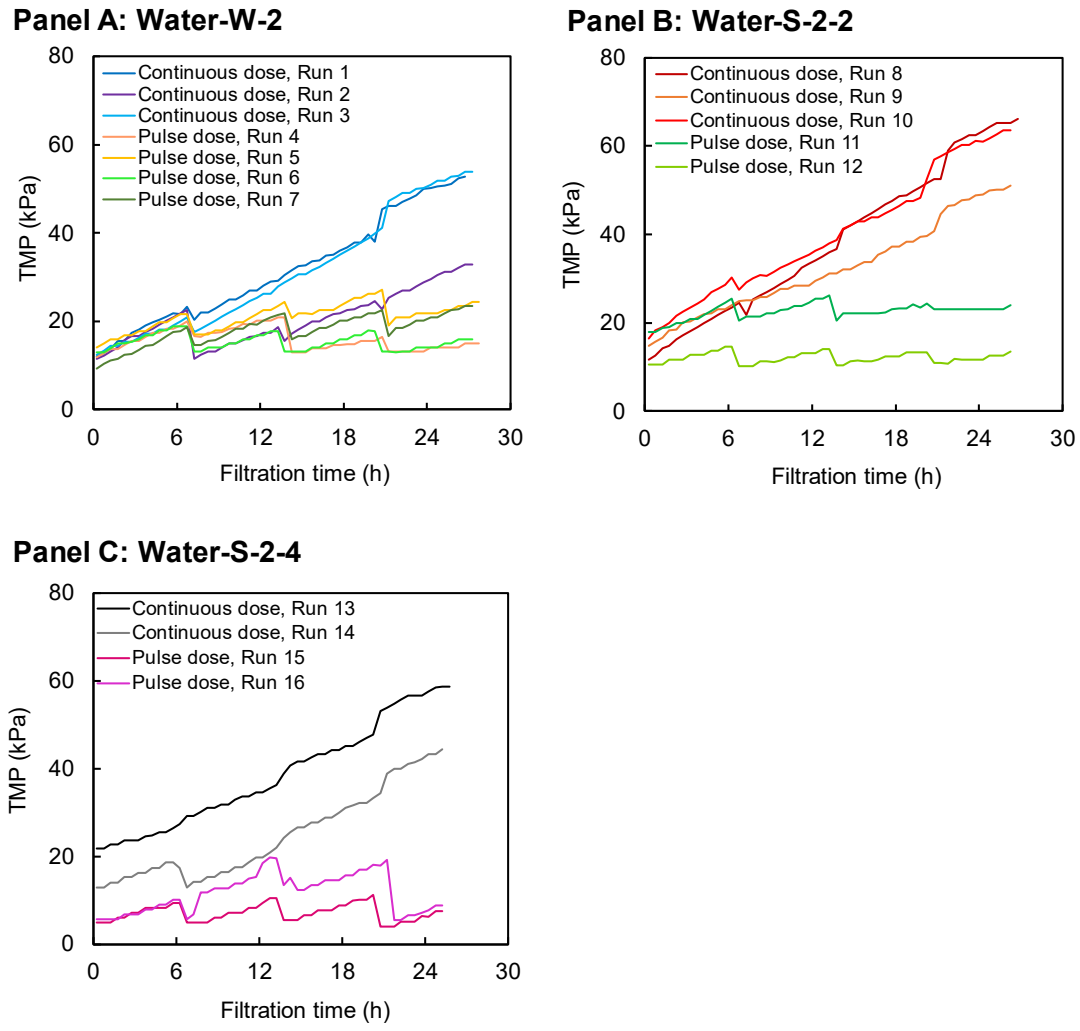

Fig. 2. Transmembrane pressure (TMP) as a function of filtration time. Filtration was conducted in a submerged ceramic membrane tank fed with water pretreated by SSPAC (submicron super-fine powdered activated carbon) adsorption and coagulation. SSPAC was dosed continuously or in a pulse after each backwash. The backwash interval was 7 h. The filtration rate was 1.93 m/day (80.4 L m^{-2} h^{-1}). Water-W-2 (Panel A), Water-S-2-2 (Panel B), and Water-S-2-4 (Panel C) were used.

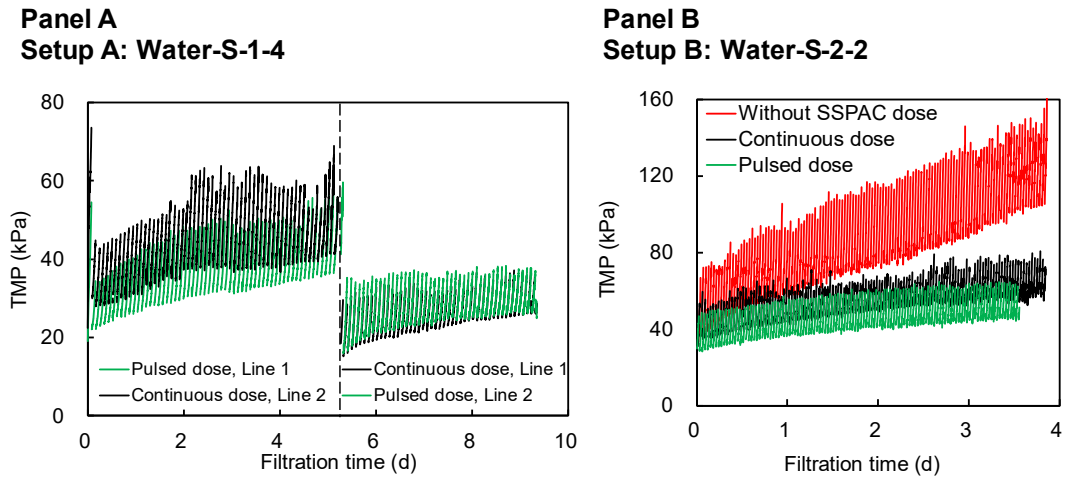

Fig. 3. Transmembrane pressure (TMP) as a function of filtration time. Filtration was conducted in a monolithic ceramic membrane system after SSPAC (submicron super-fine powdered activated carbon) adsorption and coagulation pretreatment. SSPAC was dosed continuously or in pulses. The filtration rate and backwash interval were 5 m/d (208 L m^{-2} h^{-1}) and 2 h for Panel A and 10.5 m/d (438 L m^{-2} h^{-1}) and 0.63 h for Panel B. Water-S-1-4 (Panel A) and Water-S-22 (Panel B) were used. For the Panel A experiment, coagulant and SSPAC dosages were controlled at 1 mg-Al/L and 2 mg/L during operation days 0–5 and 0.5 mg-Al/L and 1 mg/L during operation days 5–9, respectively. For the Panel B experiment, coagulant and SSPAC dosages were controlled at 1 mg-Al/L and 2 mg/L, respectively.

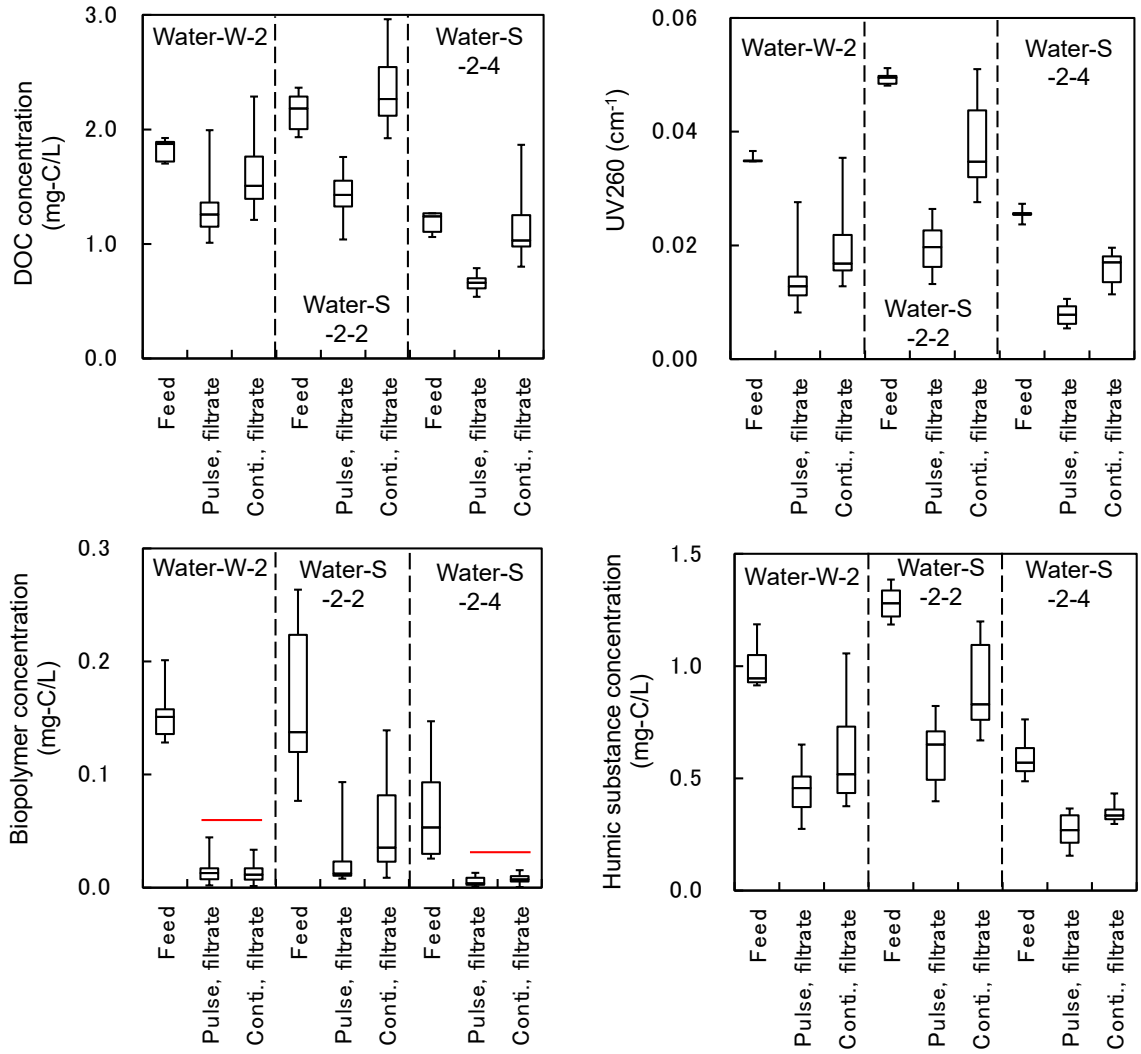

Fig. 4. Box-and-whisker plots of concentrations of dissolved organic carbon (DOC), ultraviolet absorbance at 260 nm (UV260), biopolymers, and humic substances in feedwater and filtrates after pulse and continuous dosing of submicron super-fine powdered activated carbon (SSPAC) in the case of a submerged membrane (designated as Feed, Pulse, and Conti., respectively, in this figure). Horizontal lines within boxes represent median values; the upper and lower horizontal lines of the boxes represent the 75th and 25th percentiles, respectively, and the upper and lower bars outside the boxes indicate the maximum and minimum values, respectively. The red bars over boxes indicate no significant differences ($p > 0.05$) based on a Student's *t*-test.

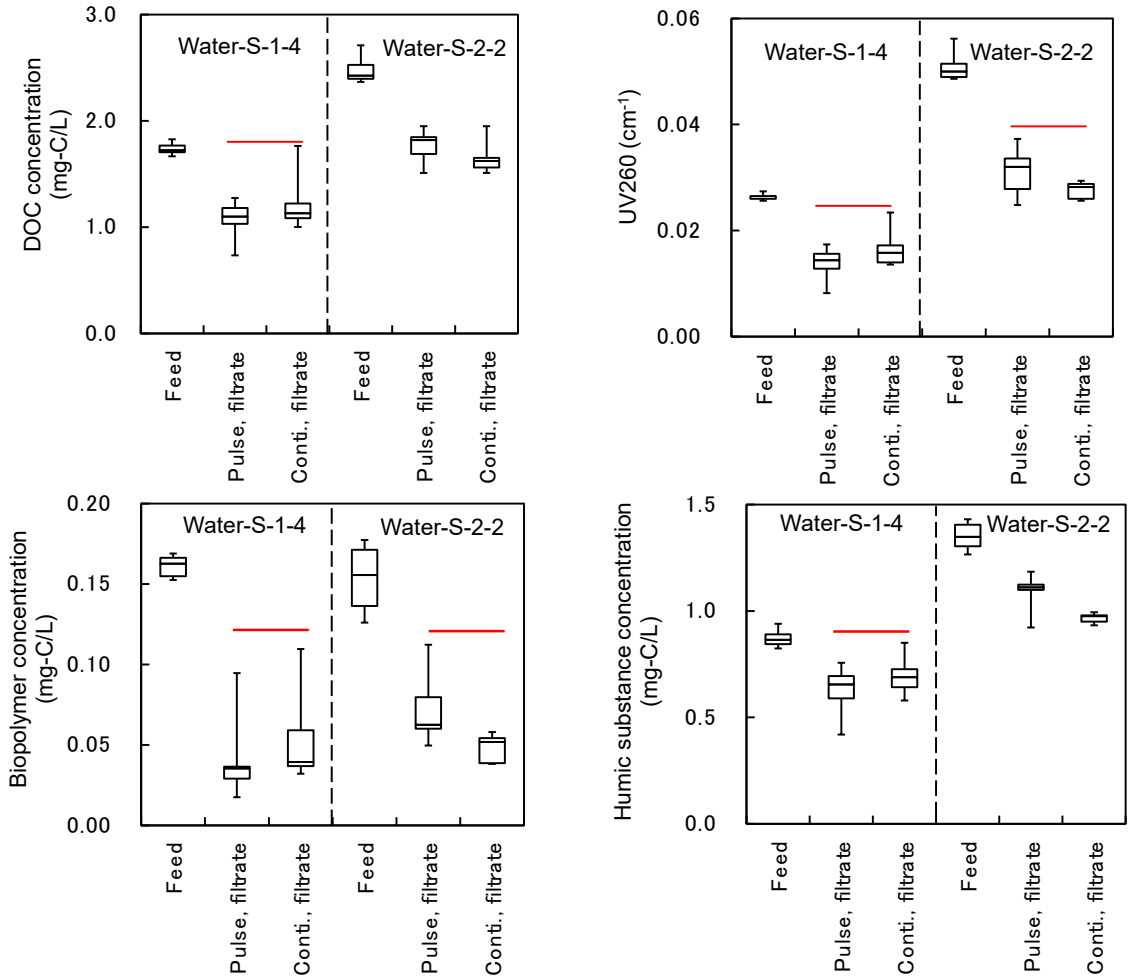

Fig. 5. Box-and-whisker plots of concentrations of dissolved organic carbon (DOC), ultraviolet absorbance at 260 nm (UV260), biopolymers, and humic substances in feedwater and filtrates after pulse and continuous dosing of submicron super-fine powdered activated carbon (SSPAC) in the case of monolithic membrane filters (designated as Feed, Pulse and Conti. in the figure, respectively). Horizontal lines within boxes represent median values, the upper and lower horizontal lines in the boxes represent the 75th and 25th percentiles, respectively. The upper and lower bars outside the boxes indicate the maximum and minimum values, respectively. Red bars over boxes indicate no significant differences ($p > 0.05$) based on a Student's *t*-test.

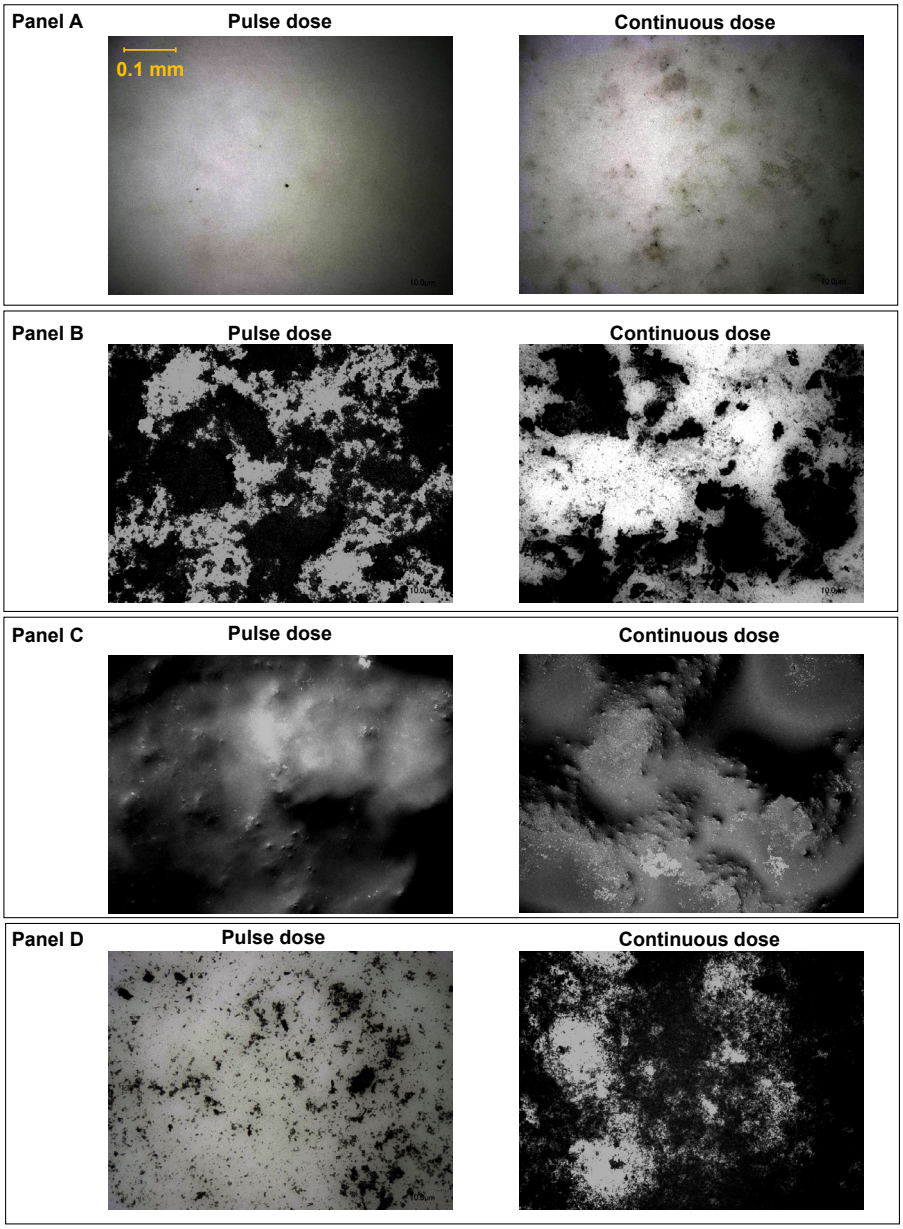

Fig. 6. Photomicrographs of the surface of the submerged ceramic membrane (500-fold magnification). Panel A shows pictures of membranes before filtration. Panel B shows pictures of membranes after a 30-min filtration. Panel C shows pictures of membranes after a 7-h filtration, which took place immediately before the backwash. Panel D shows pictures of membranes immediately after backwashing. The submicron super-fine powdered activated carbon (SSPAC) was dosed in a pulse or dosed in a continuous. The backwash was conducted at 50 kPa for 30 s. The filtration rate was 1.93 m/d (80.4 L m^{-2} h^{-1}). Water-S-2-4 was used in this experiment.

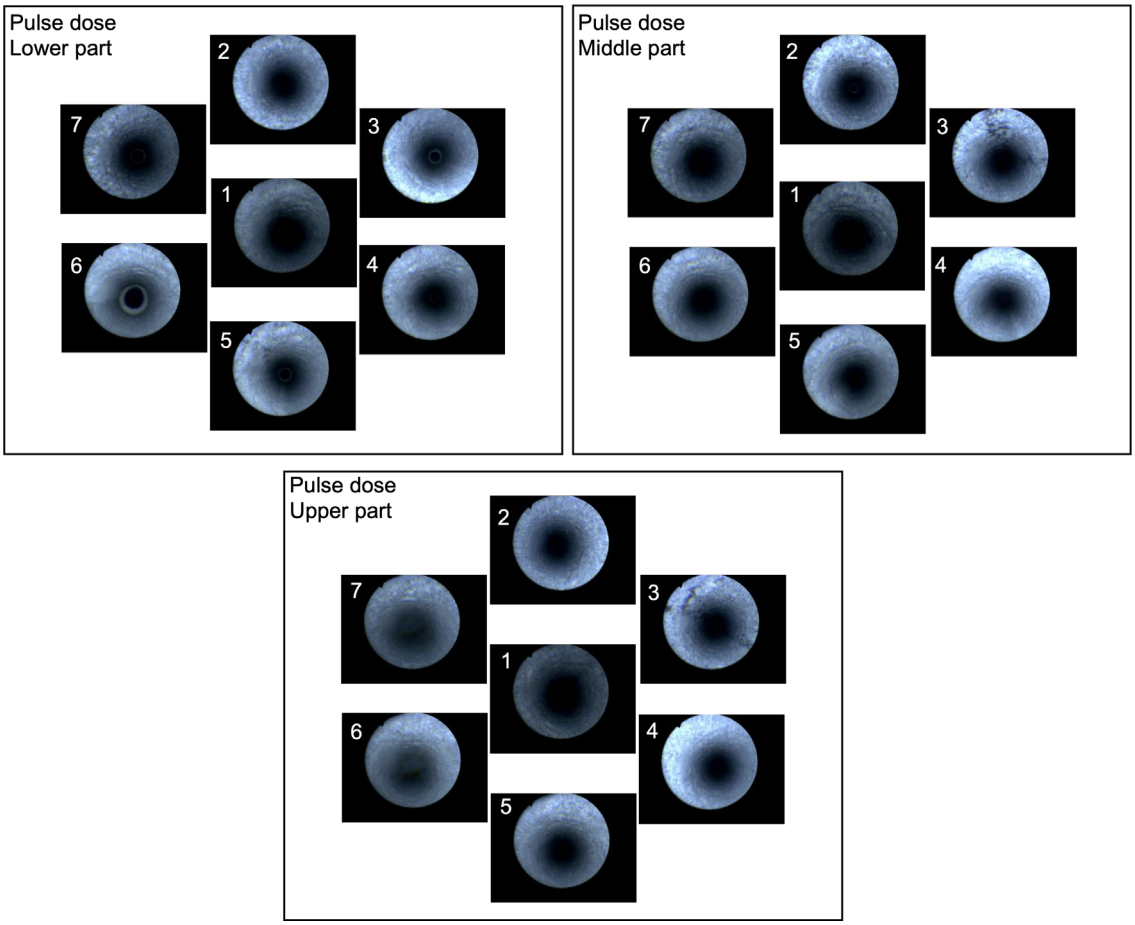

Fig. 7. Photographs of the insides of channels in a monolithic ceramic membrane taken by a fiber microscope (Observation-2). The membrane (Membrane-1) was removed at a filtration time of 5 min after a pulse dose of submicron super-fine powdered activated carbon (SSPAC). The locations of the channel areas (lower part, middle part, and upper part) and numbers that identify the channel locations are presented in Figure 11S of the SI. The filtration rate was 10.5 m/d (438 L m^{-2} h^{-1}). Water-S-3-2 was used.

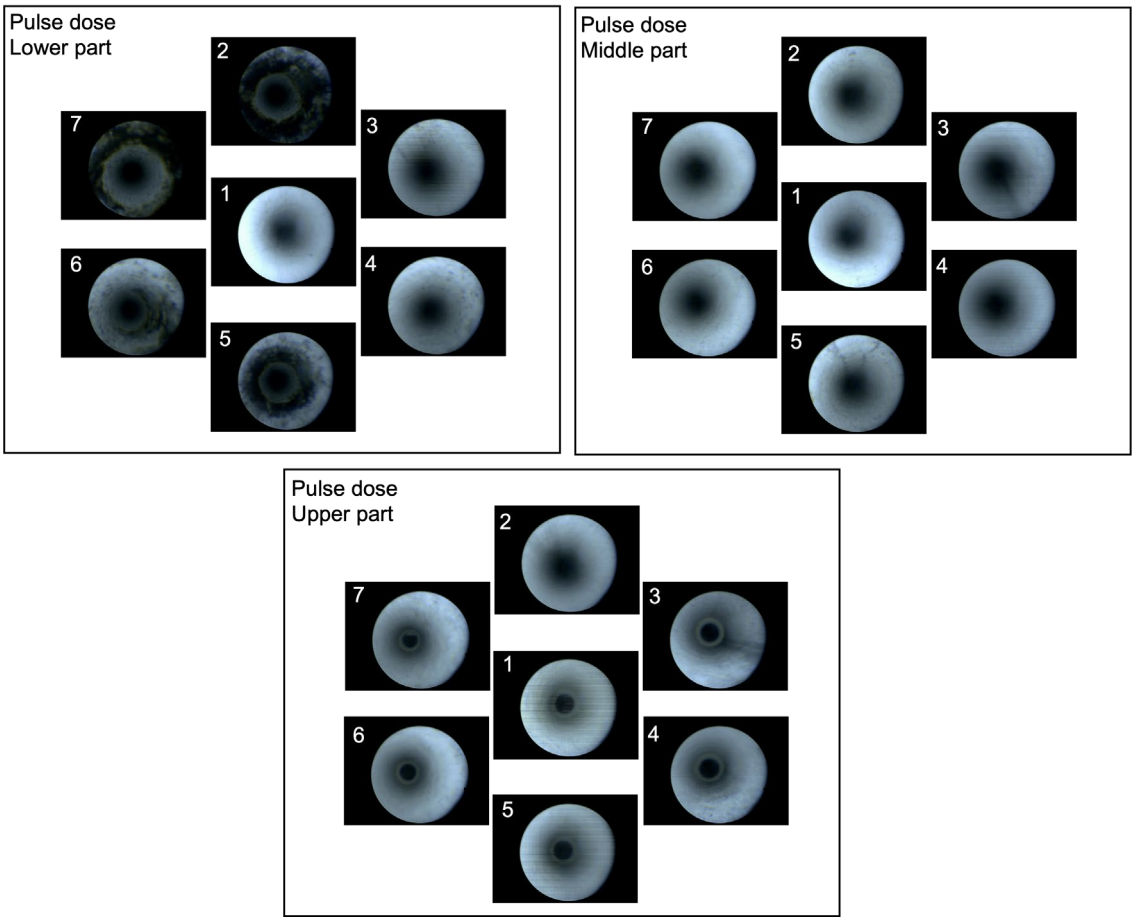

Fig. 8. Photographs of the inside of channels in a monolithic ceramic membrane taken under a fiber microscope (Observation-6). The membrane (Membrane-4) was taken out after a 5-min filtration in the experiments with a pulse dose of submicron super-fine powdered activated carbon (SSPAC). The locations of the channel areas (lower part, middle part, and upper part) and numbers that identify the channel locations are presented in Figure 11S of the SI. The filtration rate was 10.5 m/d (438 L m^{-2} h^{-1}). Water-S-3-2 was used.

Supplementary Data

Effectiveness of pulse dosing of submicron super-fine powdered activated carbon in preventing transmembrane pressure rise in outside-in-type tubular and inside-out-type monolithic ceramic membrane microfiltrations

Yuanjun Zhao [a], *Yoshihiko Matsui* [b,*], *Shun Saito* [a], *Nobutaka Shirasaki* [b], *Taku Matsushita* [b]

[a] *Graduate School of Engineering, Hokkaido University, N13W8, Sapporo, 060-8628, Japan*

[b] *Faculty of Engineering, Hokkaido University, N13W8, Sapporo, 060-8628, Japan*

* *Corresponding author*. Tel/fax: +81-11-706-7280

E-mail address: matsui@eng.hokudai.ac.jp (Y. Matsui)

Text 1S

The DOC concentration was measured with a TOC analyzer (Model 900, Sievers Instruments, Boulder, CO, USA). The UV260 was measured using a UV spectrophotometer (UV-1800, Shimadzu, Kyoto, Japan). We configured a size-exclusion chromatography–organic carbon detection system similar to the system originally developed by Huber et al. (2011) to analyze the concentrations of biopolymers and HS: a high-performance liquid chromatography (HPLC) system (1100 series, Agilent Tech, Tokyo, Japan) consisting of a single column (Toyopearl HW-50S, 250 mm × 20 mm, Tosoh Inc., Tokyo, Japan), an injection system (flux of 1.2 mL/min), a UV detector, and a TOC analyzer (M9e, Central Kagaku Corp., Tokyo, Japan). The HS were treated as a group that also included the building blocks because the HS and the building blocks partly overlapped each other [30]. However, the HS were much larger in chromatograms, as shown in Figure 1S of the SI.

Text 2S

We applied a model to quantify the change of TMP as a function of time [49].

$$P_L = \alpha\mu c_s \frac{Q^2}{A^2} t + \mu R_c \frac{Q}{A} \qquad (1S)$$

where P_L is transmembrane pressure (Pa), α is specific cake resistance (m/kg, constant in the case of incompressible cake layer) and c_s is solid volume fraction of the suspension being filtrated (kg/m^3), Q is volumetric flow rate (m^3/s), A is filter cross-sectional area (m^2), t is time (s), μ is fluid viscosity (Pa·s) and R_c is cake resistance (m^{-1}).

For submerged tubular ceramic membrane, data from Panel B in Fig. 2 was used for calculating the slope and intercept. For monolithic ceramic membrane, data from Panel B in Fig. 3 was used and the calculated parameter is shown in Table 4S of the SI. Pulse dosing of SSPAC achieves much smaller slope and intercept than continuous dosing of SSPAC in the case of tubular ceramic membrane, indicating a smaller cake resistance. On the other hand, pulse dosing of SSPAC achieves a similar slope and relatively smaller intercept than continuous dosing of SSPAC in the case of monolithic membrane, indicating that at the point of t=0, the initial TMP of pulse dosing of SSPAC is slightly smaller while no significant differences during the filtration than continuous dosing of SSPAC, which can be explained as the pulse dosing of SSPAC provides sufficient SSPAC for foulants removal.

Table 1S

Feedwater quality.

	pH	DOC mg/L	UV abs. at 260 nm cm^{-1}	Biopolymer mg/L	Humic substances mg/L	Alkalinity mg/L as $CaCO_3$	Na^+ mg/L
Water-W-1	7.96	3.69	0.070	0.31	2.55	71	43.8
Water-S-1-4	7.39	1.65	0.031	0.11	1.01	19	24.5
Water-S-2-1	6.56	4.31	0.099	0.33	3.12	16	51.1
Water-S-3-1	7.00	5.19	0.100	0.67	2.14	31	42.2

	K^+ mg/L	Mg^{2+} mg/L	Ca^{2+} mg/L	Cl^- mg/L	NO_3^- mg/L	SO_4^{2-} mg/L
Water-W-1	5.55	9.25	17.9	51.6	n/a	14.8
Water-S-1-4	4.56	2.55	13.1	36.3	9.22	20.7
Water-S-2-1	10.5	4.55	17.8	58.7	41.2	25.4
Water-S-3-1	9.77	3.97	17.4	49.0	29.7	23.2

Table 2S

Operating conditions of submerged tubular and monolithic membrane systems.

Membrane system	Channels	Nominal pore size µm	Filtration area cm^2	Filtration flux m/d	Filtration flux $L\ m^{-2}\ h^{-1}$	Backwash interval h	Backwash time s	Backwash pressure kPa
Submerged tubular	1	0.1	5.30	1.93	80.4	7.0	30	50
Monolith (Setup A)	22	0.1	172	5.00	208	2.0	10	500
Monolith (Setup B)	7	0.1	54.7	10.5	438	0.63	10	500
Monolith (Setup B)	22	0.1	172	1.67	69.8	7.0	10	50

Membrane system	Channels	Mixing intensity (G value)			Detention time		
		Rapid mixing s^{-1}	Slow mixing 1 s^{-1}	Slow mixing 2 s^{-1}	Rapid mixing min	Slow mixing 1 min	Slow mixing 2 min
Submerged tubular	1	609			3.72		
Monolith (Setup A)	22	41.8	8.1	4.0	11.9	11.9	20.4
Monolith (Setup B)	7	71.8	9.4		7.70	13.2	
Monolith (Setup B)	22	110.6	17.9		15.9	27.3	

Table 3S

Specifications of the tubular ceramic membrane and the monolithic ceramic membrane from the catalogs of the manufacturers.

Membrane type	Tubular	Monolithic	Flat sheet
Maker	Kubota Corp.	Metawater Co. Ltd.	Metawater Co. Ltd.
Material	Ceramics	Ceramics	Ceramics
Nominal pore size	0.1 μm	0.1 μm	0.1 μm
Filtration direction	Outside-in	Inside-out	Upstream-downstream
Filtration pressure	Negative pressure	Positive pressure	Positive pressure
Setting	Submerged in a tank	Housed in a casing	Housed in a casing

Table 4S Parameter values of the model fitted to equation (1S). The data from Panel B in Fig. 2 was used for submerged tubular ceramic membrane, while the data from Panel B in Fig. 3 was used for monolithic ceramic membrane.

	Tubular membrane		Monolithic membrane	
	αc_s	R_c	αc_s	R_c
	10^6 m^{-2}	10^6 m^{-1}	10^6 m^{-2}	10^6 m^{-1}
Continuous dosing of SSPAC	0.89±0.20	1.42±0.68	0.54±0.11	0.39±0.06
Pulse dosing of SSPAC	0.34±0.19	0.68±0.25	0.58±0.04	0.31±0.04

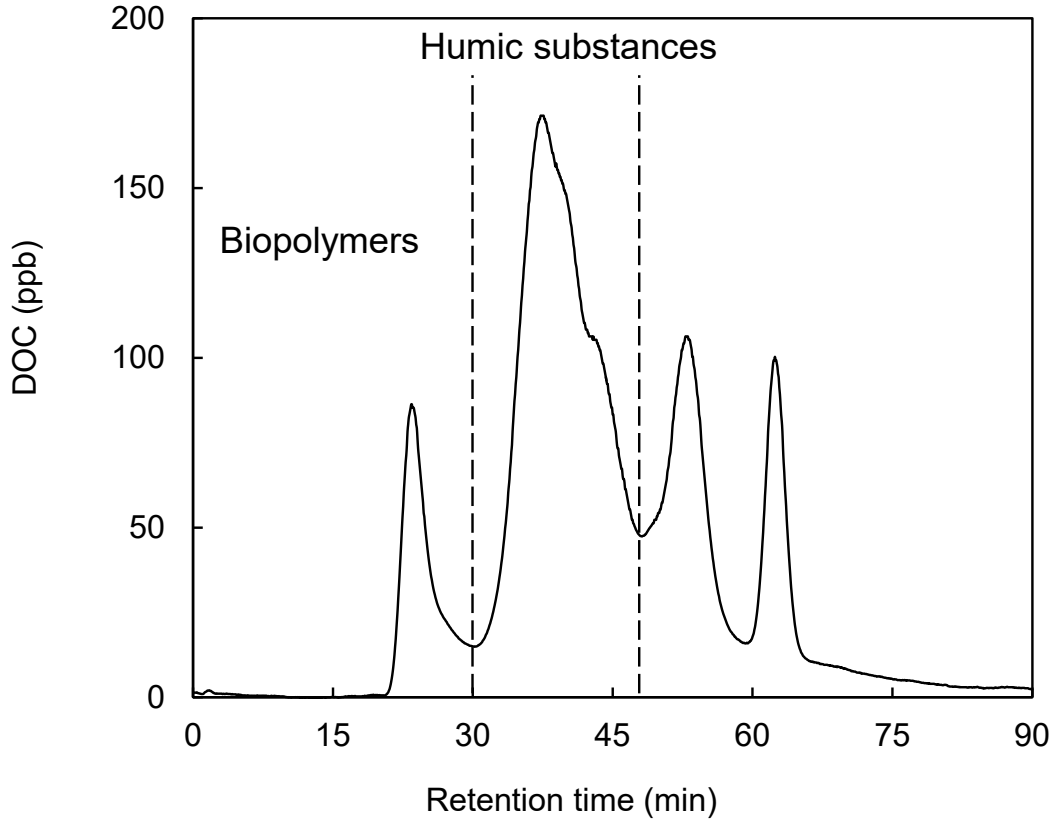

Fig. 1S. Chromatograms by size-exclusion chromatography–organic carbon detection system. Water-S-2-1 was used.

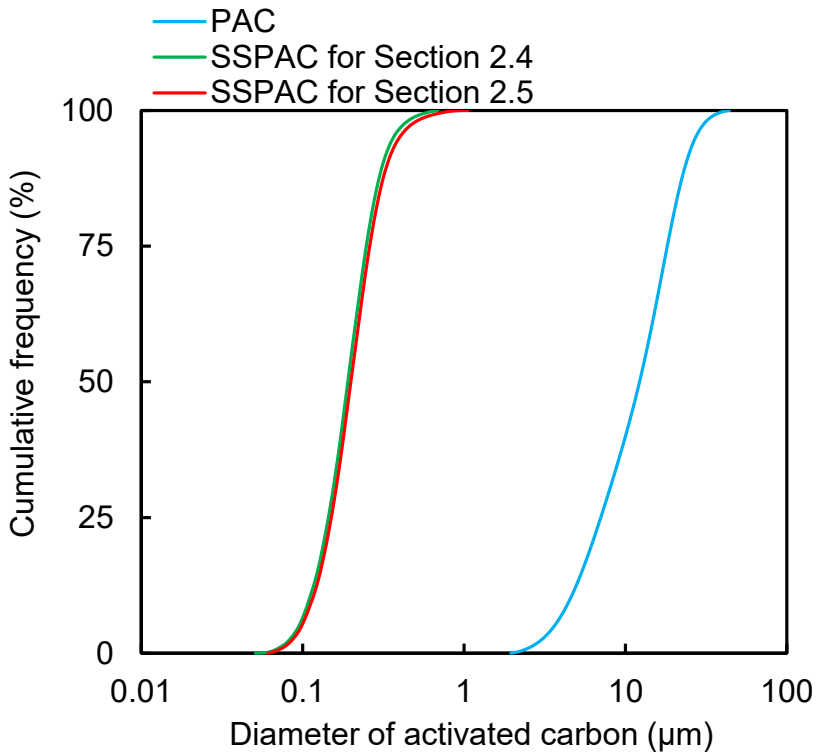

Fig. 2S. Size distributions of PAC (powdered activated carbon) and submicron super-fine PAC (SSPAC).

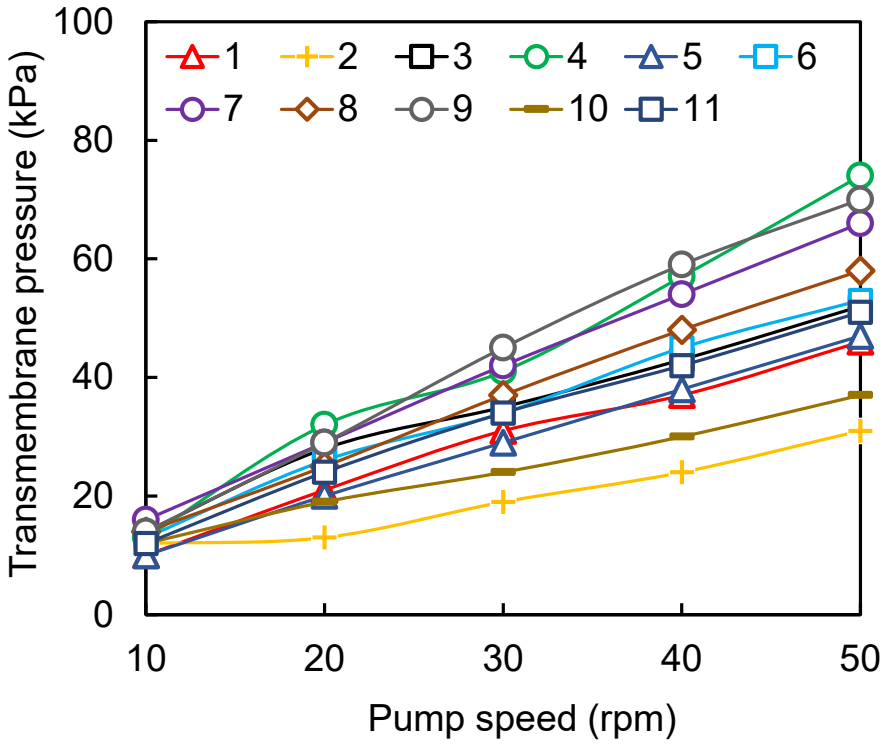

Fig. 3S. Permeability test for cut pieces of submerged tubular ceramic membranes. The pair of membrane pieces 1 and 5 and the pair of membrane pieces 3 and 11 were used in the experimental comparisons.

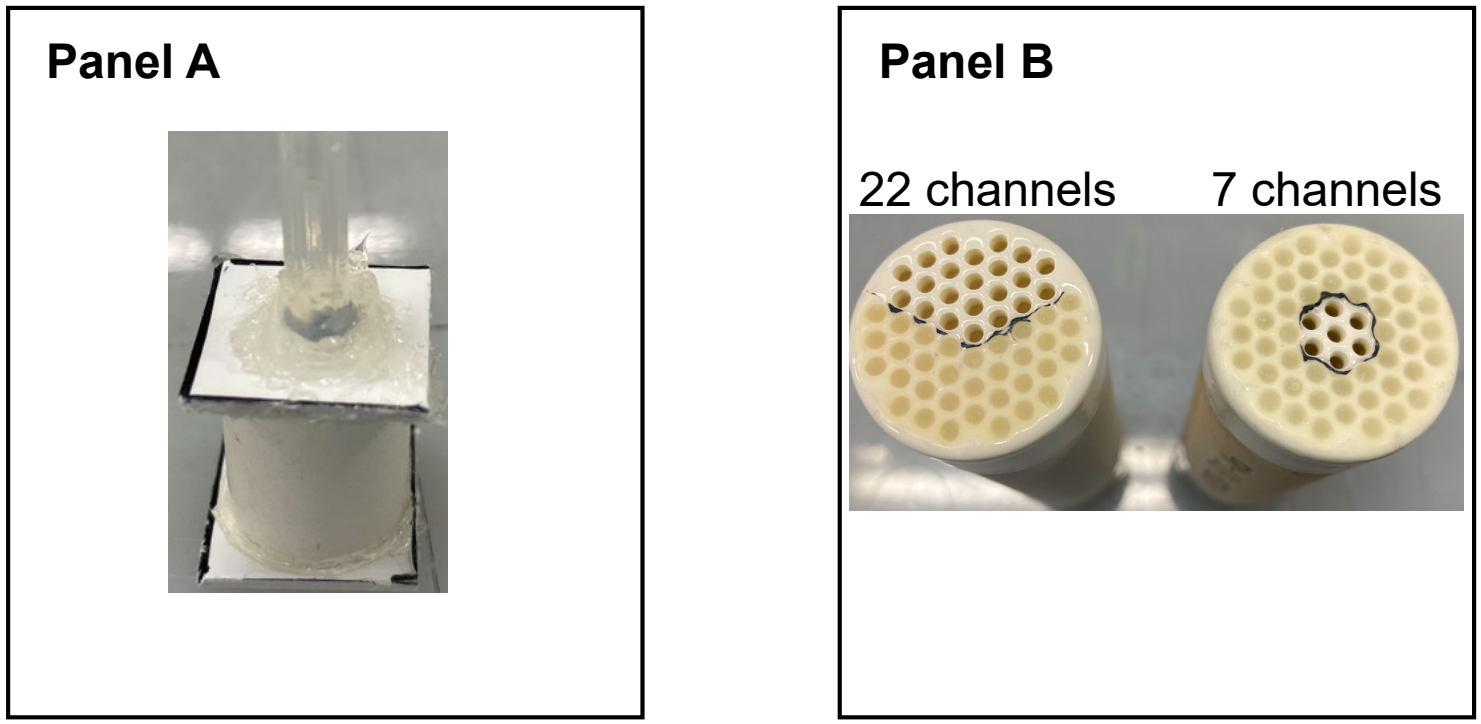

Fig. 4S. Pictures of the geometries of a submerged membrane element (Panel A) and monolithic membrane elements (Panel B).

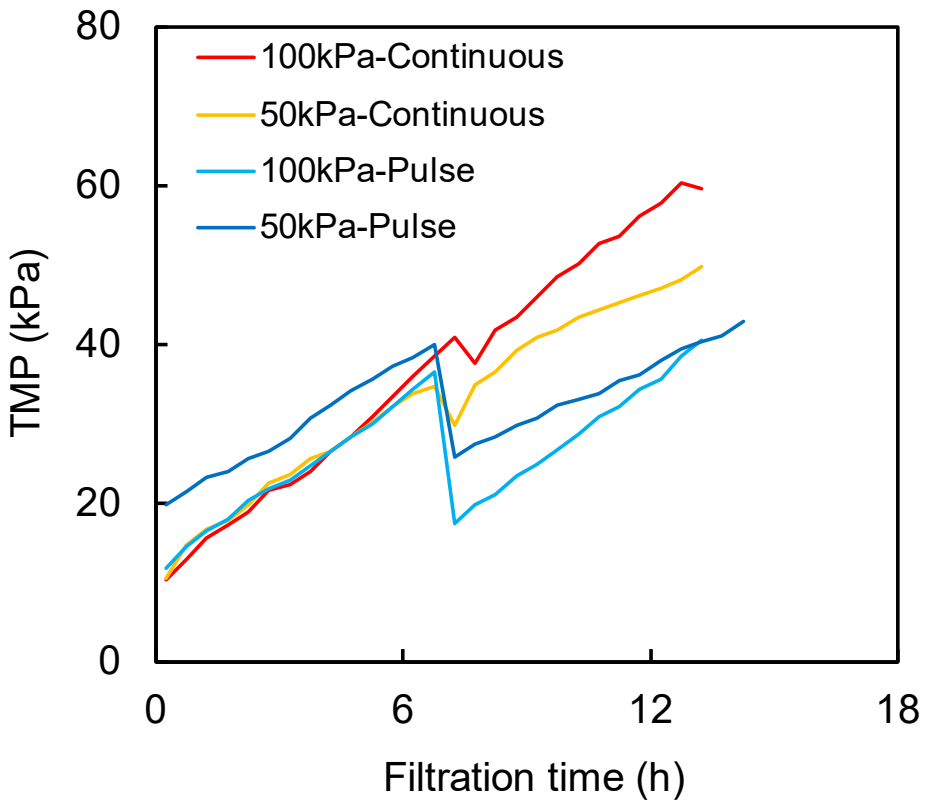

Fig. 5S. Transmembrane pressure (TMP) as a function of filtration time. Filtration was conducted in a submerged-tubular ceramic membrane tank fed with water pretreated by submicron super-fine powdered activated carbon (SSPAC) adsorption and coagulation. The SSPAC was dosed continuously or in pulses. Backwash interval was 7 h. Filtration rate was 1.93 m/d (80.4 L m^{-2} h^{-1}). Backwash pressure was applied from a pressure tank at 100 kPa or 50 kPa. Water-S-3-2 was used.

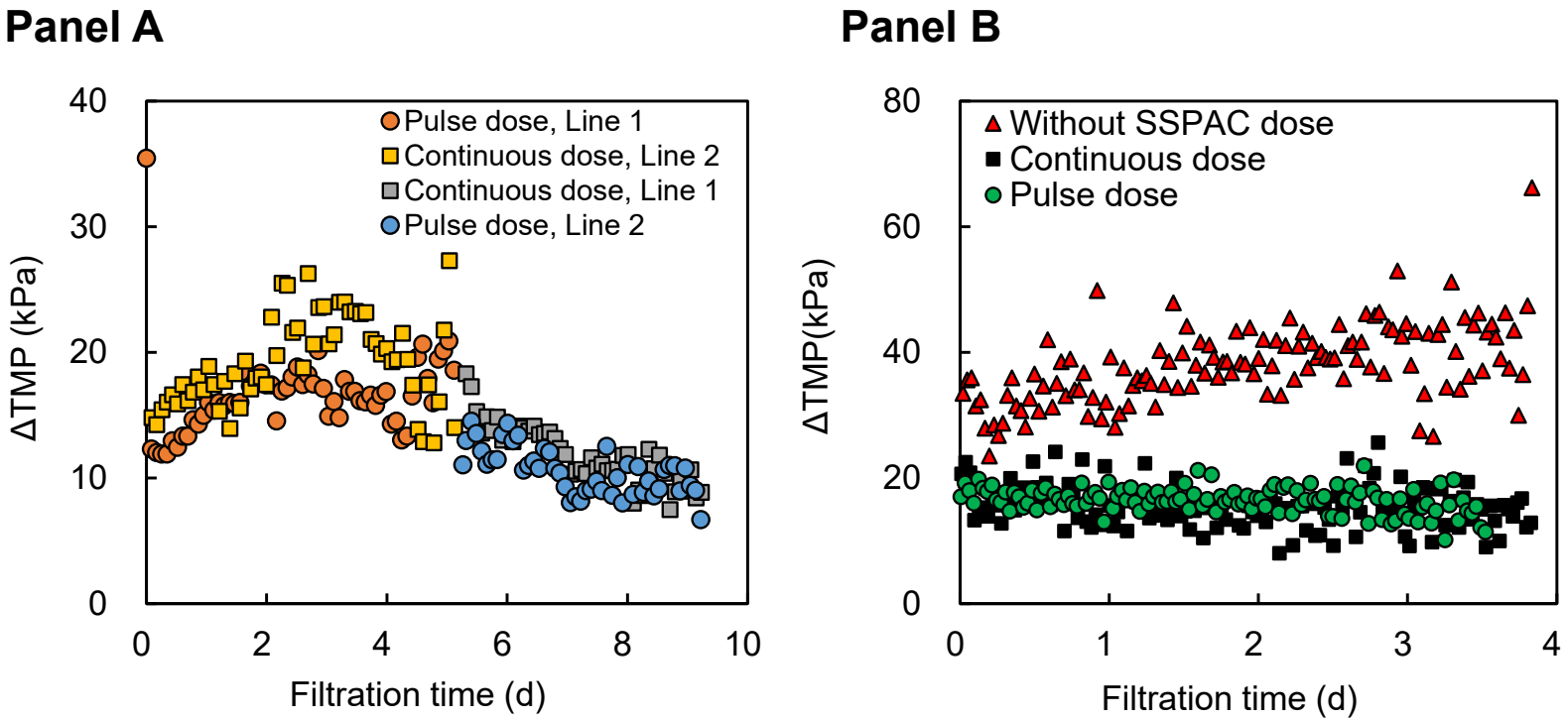

Fig. 6S. ΔTMP (increase of transmembrane pressure during one batch of filtration after backwash) as a function of filtration time. Filtration was conducted in a monolithic ceramic membrane system after submicron super-fine powdered activated carbon (SSPAC) adsorption and coagulation pretreatment. SSPAC was dosed continuously or in pulses. The filtration rate and backwash interval were 5 m/d (208 L m^{-2} h^{-1}) and 2 h for Panel A and 10.5 m/d (438 L m^{-2} h^{-1}) and 0.63 h for Panel B. Water-S-1-4 (Panel A) and Water-S-2-2 (Panel B) were used. For panel A, coagulant and SSPAC dosages were controlled at 1 mg-Al/L and 2 mg/L during operation days 0–5, and 0.5 mg-Al/L and 1 mg/L during operation days 5–9, respectively. For panel B, coagulant and SSPAC dosages were controlled at 1 mg-Al/L and 2 mg/L.

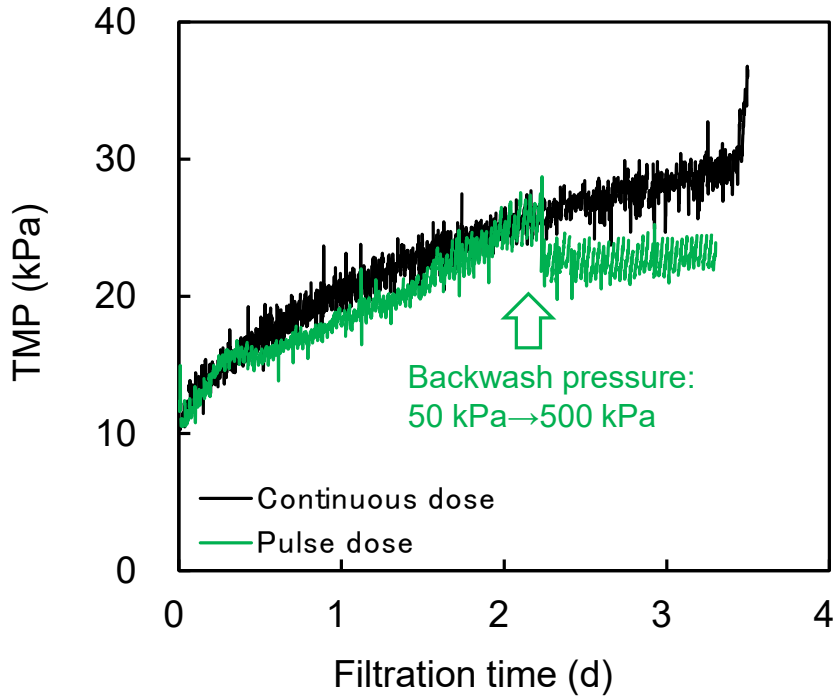

Fig. 7S. Transmembrane pressure (TMP) as a function of filtration time. After submicron super-fine powdered activated carbon (SSPAC) adsorption and coagulation pretreatment, filtration was conducted in the monolithic ceramic membrane system of Setup B. SSPAC was dosed continuously or in pulses. Backwash interval was 0.63 h. Filtration rate was 3.34 m/d (139 L m^{-2} h^{-1}). Water-S-3-2 was used in this experiment. Backwash pressure of the pulse dosing run was changed from 50 to 500 kPa at 2.2 days, whereas that of the continuous dosing run was kept at 50 MPa.

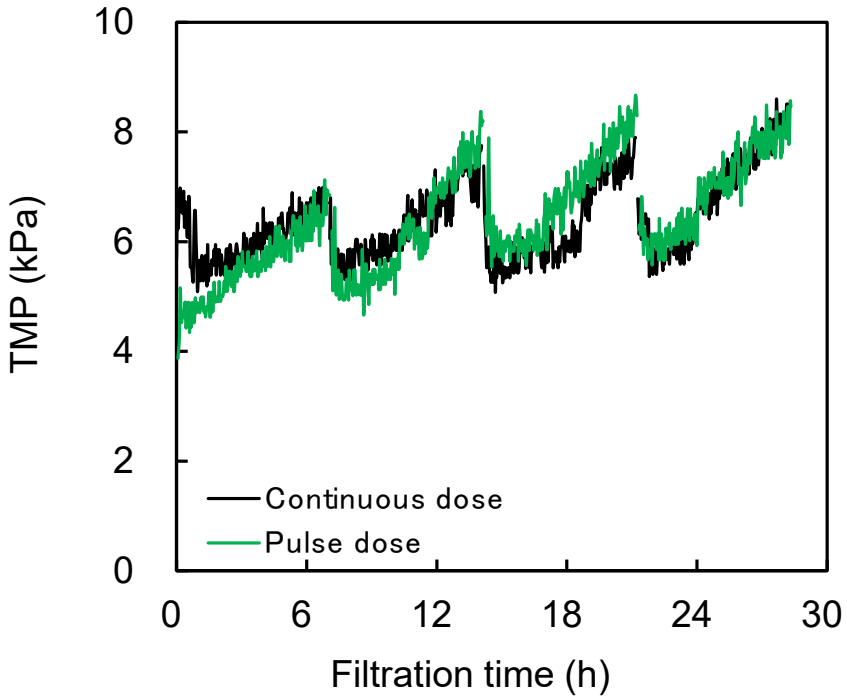

Fig. 8S. Transmembrane pressure (TMP) as a function of filtration time when filtration was conducted after submicron super-fine powdered activated carbon (SSPAC) adsorption and coagulation pretreatment in a monolithic ceramic membrane system. The experiments were conducted by pulse dosing of SSPAC using Setup B (Fig. 1) but with 22-channel membranes. Backwash interval was 7 h, and the pressure was controlled at 50 kPa. Filtration rate was 1.67 m/d (69.8 L m^{-2} h^{-1}). Water-S-3-2 was used.

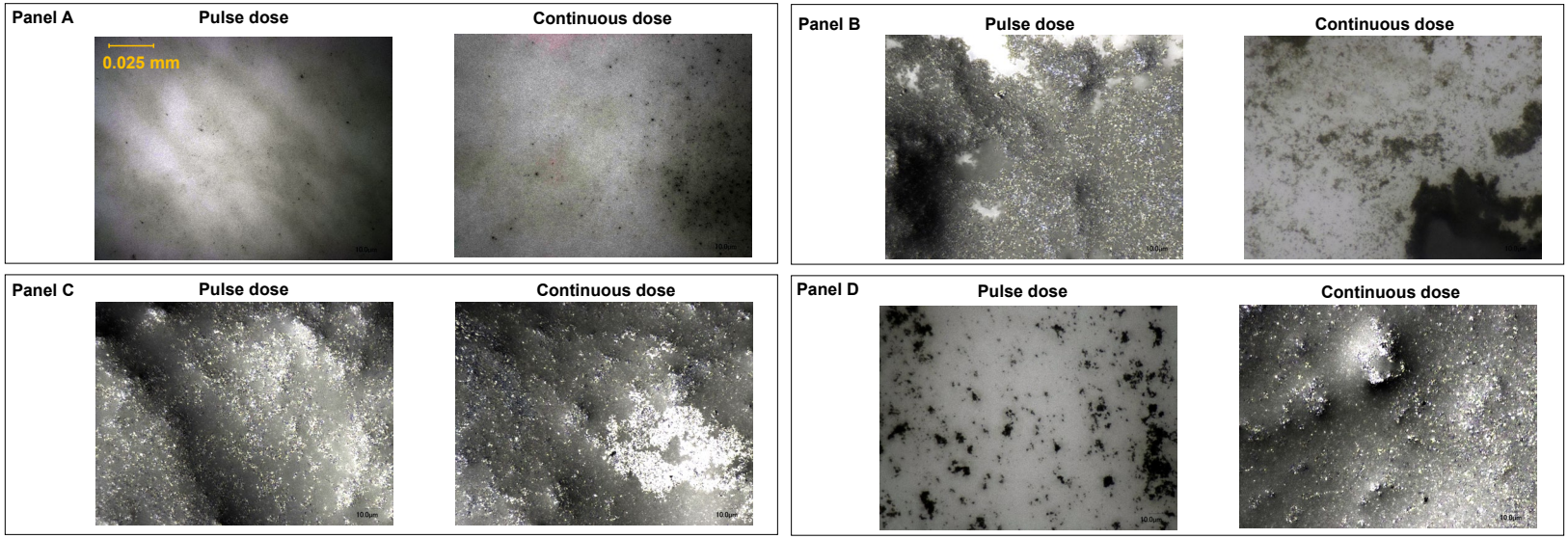

Fig. 9S. Photomicrographs of the surface of submerged-tubular ceramic membrane (magnification by 2000×). Panel A shows pictures of membranes before filtration. Panel B shows pictures of membranes after a 30-min filtration. Panel C shows pictures of membranes after a 7-h filtration, which was right before hydraulic backwashing. Panel D shows the membranes right after hydraulic backwashing. Submicron super-fine powdered activated carbon was dosed in a pulse or dosed in a continuous. Hydraulic backwash was conducted at 50 kPa for 30 s. Filtration rate was 1.93 m/d (80.4 L m^{-2} h^{-1}). Water-S-2-4 was used in this experiment.

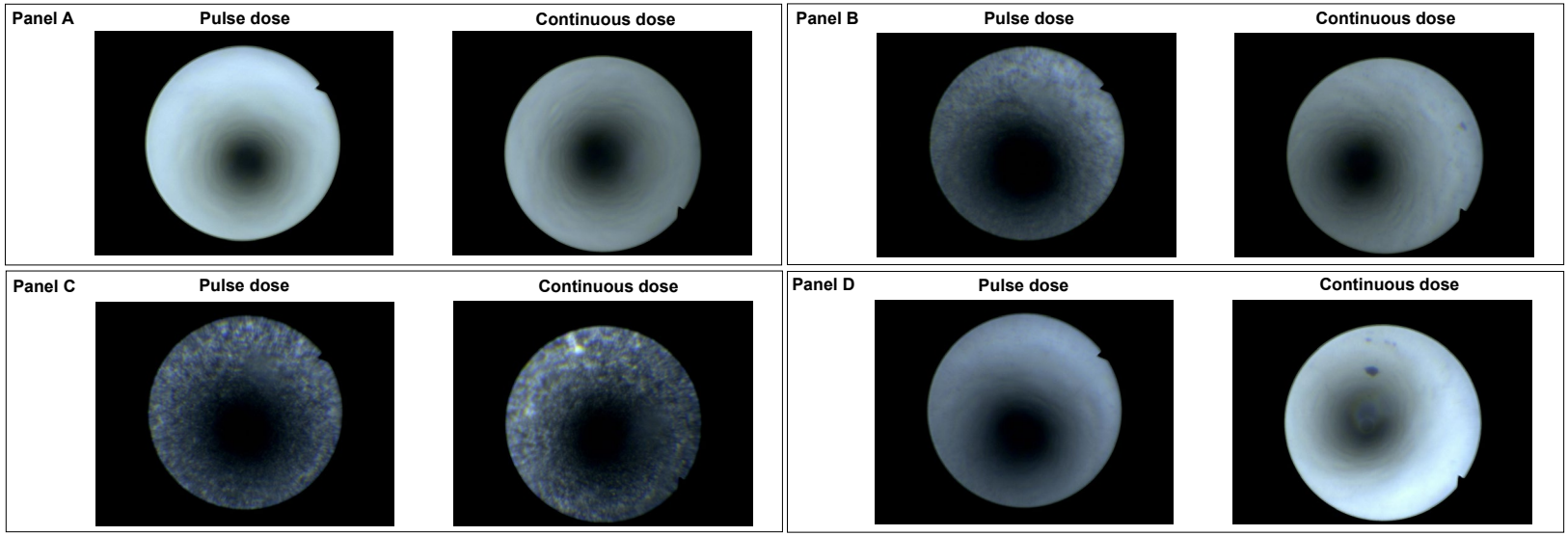

Fig. 10S. Photographs (Observation 1) of the inside of channels in a monolithic ceramic membrane taken under a fiber microscope. Panel A shows the membranes before filtration. Panel B shows the membranes after a 5-min filtration. Panel C shows the membranes after a 0.63-h filtration, which was right before hydraulic backwashing. Panel D shows the membranes right after hydraulic backwashing. The middle part of channel no. 1 of the membrane element (see Figure 11S of SI) in Setup B was observed. SSPAC was dosed in a pulse or dosed in a continuous. Hydraulic backwashing was conducted at 500 kPa for 10 s. Filtration rate was 10.5 m/d (438 L m^{-2} h^{-1}). Water-S-2-2 was used.

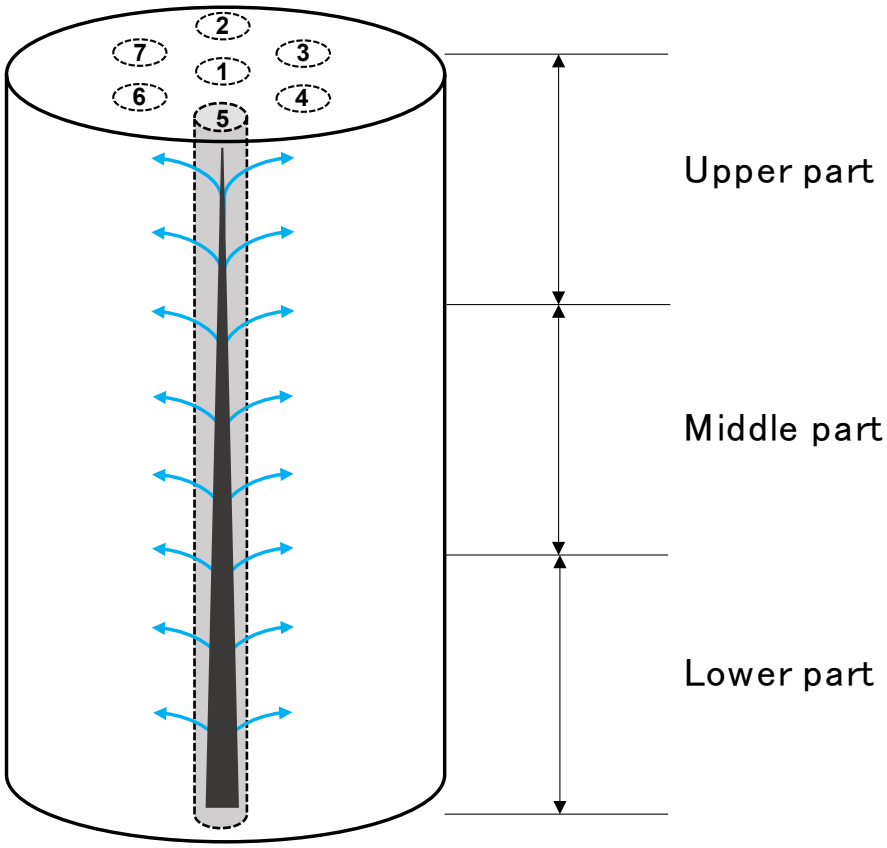

Fig. 11S. Schematic of monolithic membrane indicating filtration direction and channels. The numbers indicate channel locations. Blue arrows indicate the direction of water flow in a membrane element.

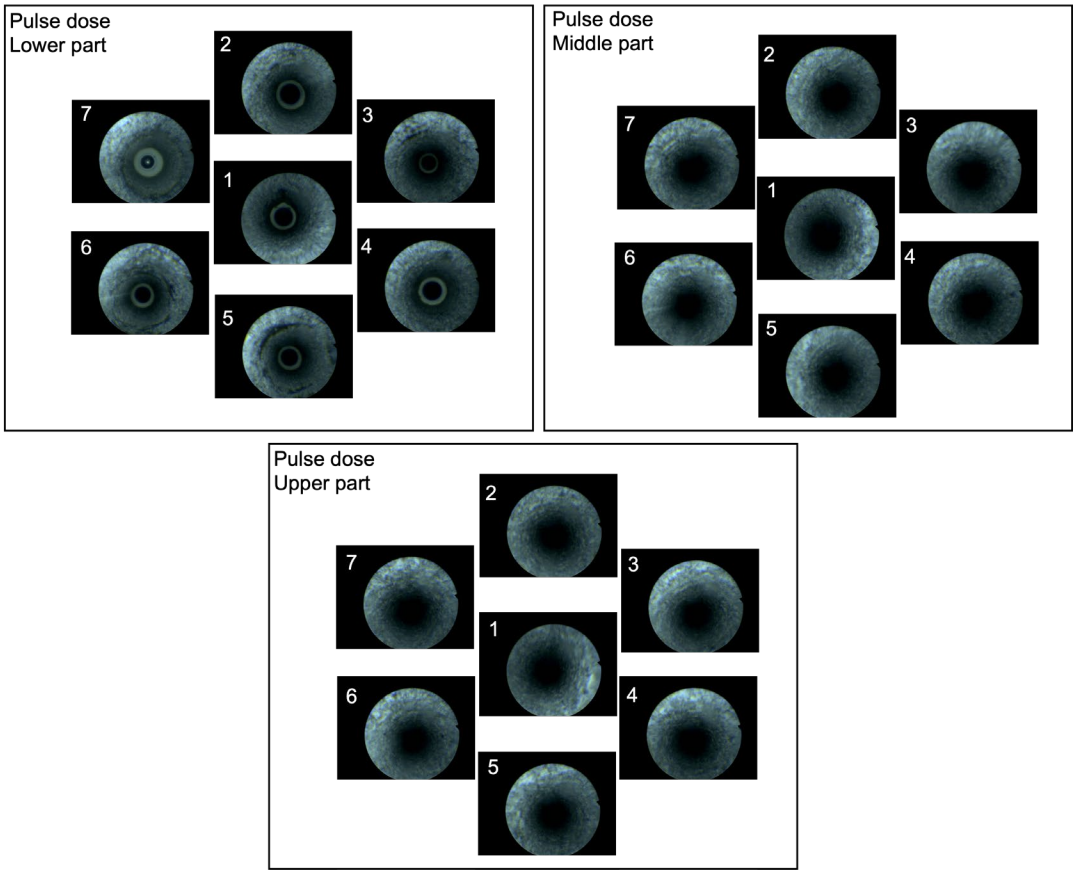

Fig. 12S. Photographs of the insides of channels in a monolithic ceramic membrane taken under a fiber microscope. Observation-3 corresponds to the membrane's (Membrane-1) being taken out after a filtration of 5 min in the experiments with a pulse dose of SSPAC. The locations of the channel areas (lower part, middle part, and upper part) and numbers are shown in Fig. 11S of the SI. Filtration rate was 10.5 m/d (438 L m^{-2} h^{-1}). Water-S-3-2 was used.

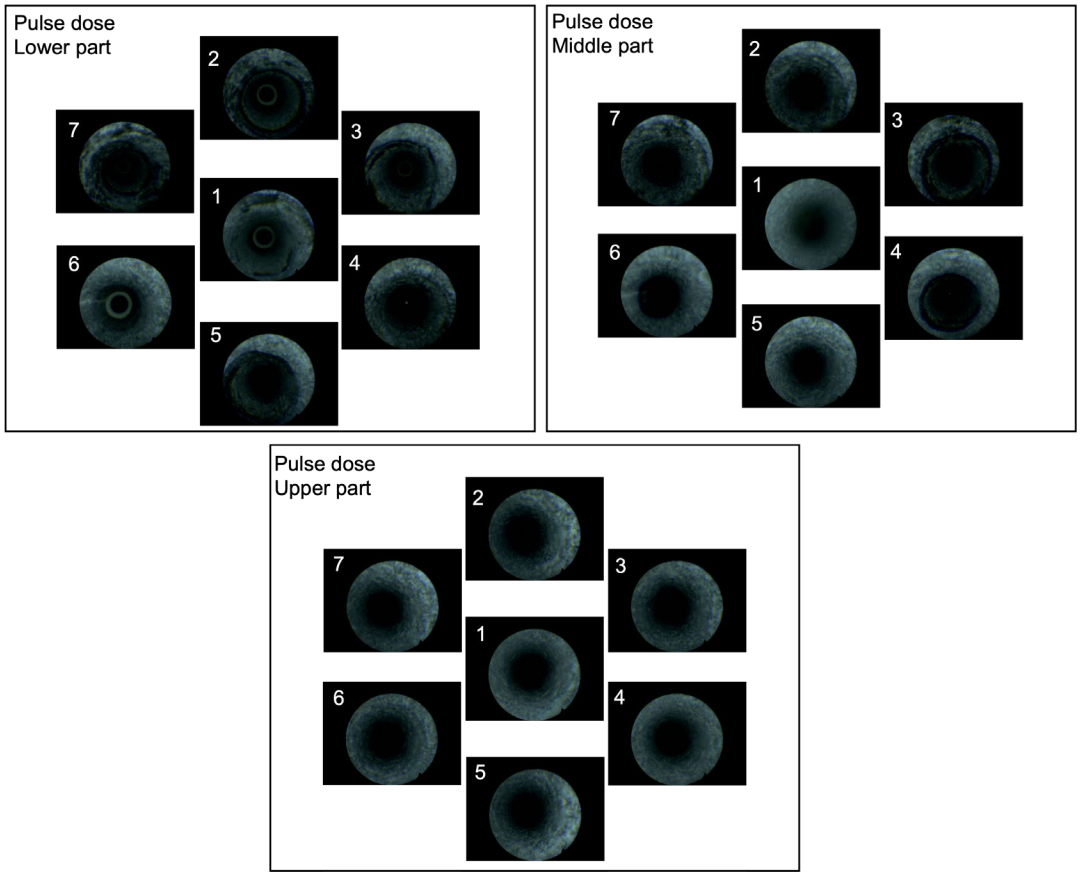

Fig. 13S. Photographs of the insides of channels in a monolithic ceramic membrane taken under a fiber microscope. Observation-4 corresponds to the membrane's (Membrane-2) being taken out after a filtration of 5 min in the experiments with a pulse dose of submicron super-fine powdered activated carbon. The locations of the channel areas (lower part, middle part, and upper part) and numbers are presented in Fig. 11S of the SI. Filtration rate was 10.5 m/d (438 L m^{-2} h^{-1}). Water-S-3-2 was used.

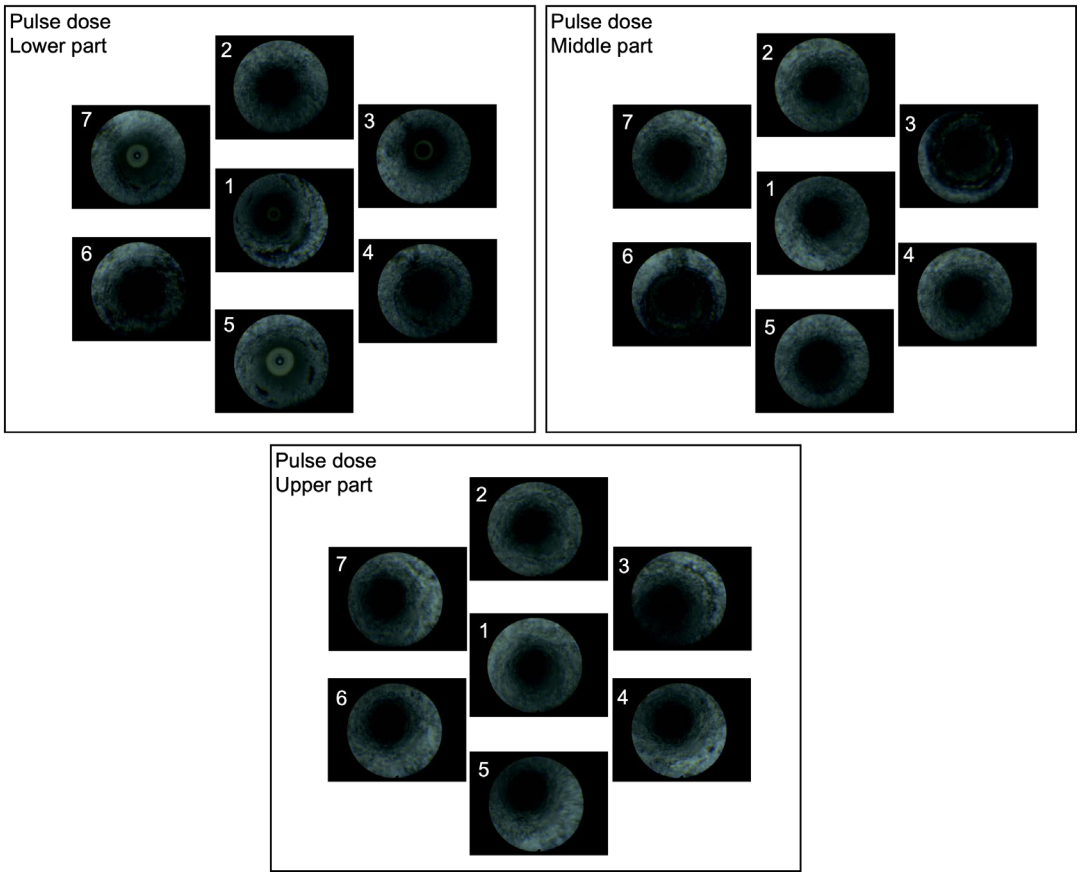

Fig. 14S. Photographs of the insides of channels in a monolithic ceramic membrane taken under a fiber microscope. Observation-5 corresponds to the membrane's (Membrane-3) being taken out after a filtration time of 5 min in the experiments with a pulse dose of submicron super-fine powdered activated carbon. The locations of the channel areas (lower part, middle part, and upper part) and numbers are presented in Fig. 11S of the SI. Filtration rate was 10.5 m/d (438 L m^{-2} h^{-1}). Water-S-3-2 was used.

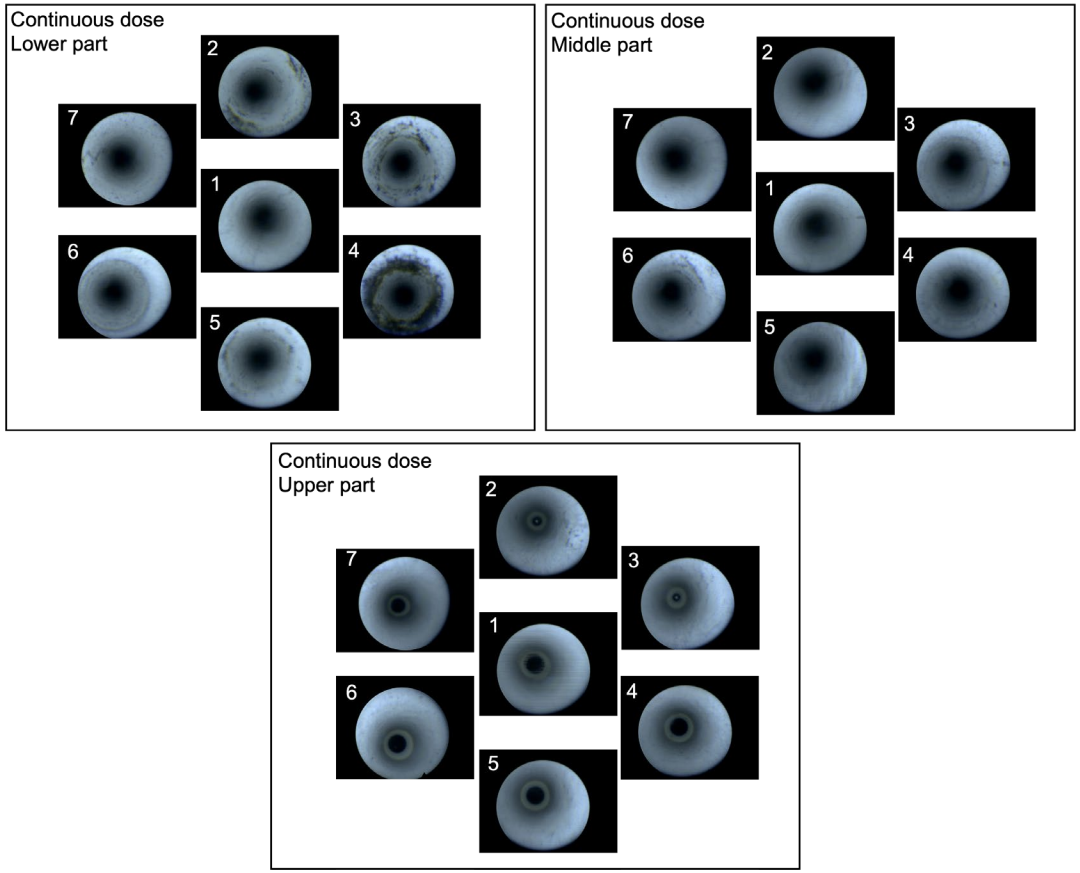

Fig. 15S. Photographs of the insides of channels in a monolithic ceramic membrane taken under a fiber microscope. Observation-7 corresponds to the membrane's (Membrane-5) being taken out after a filtration time of 5 min in the experiments with a continuous dose of submicron super-fine powdered activated carbon. The locations of the channel areas (lower part, middle part and upper part) and numbers are presented in Figure 11S of SI. Filtration rate was 10.5 m/d (438 L m^{-2} h^{-1}). Water-S-3-2 was used.

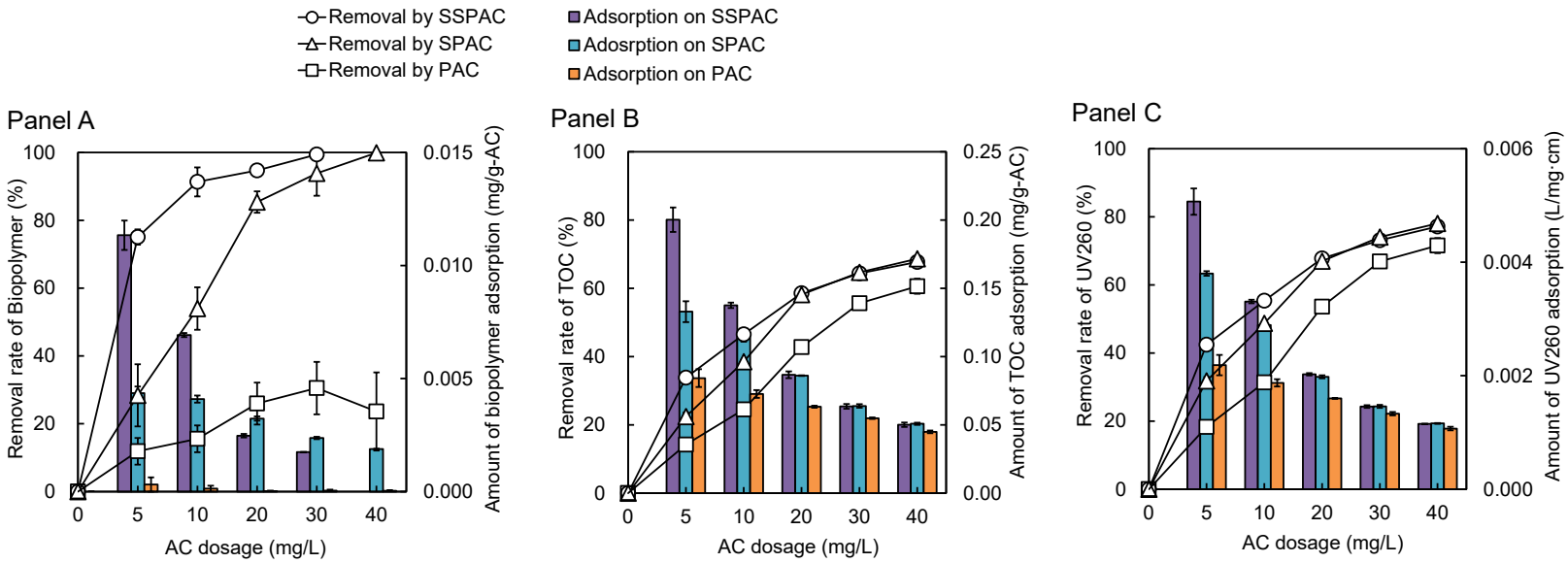

Fig. 16S. Removal rate and adsorption amount of Biopolymer (Panel A), TOC (Panel B) and UV260 (Panel C) as a function of AC dosage. Adsorption isotherm experiment was conducted at room temperature (20ºC) for one week.

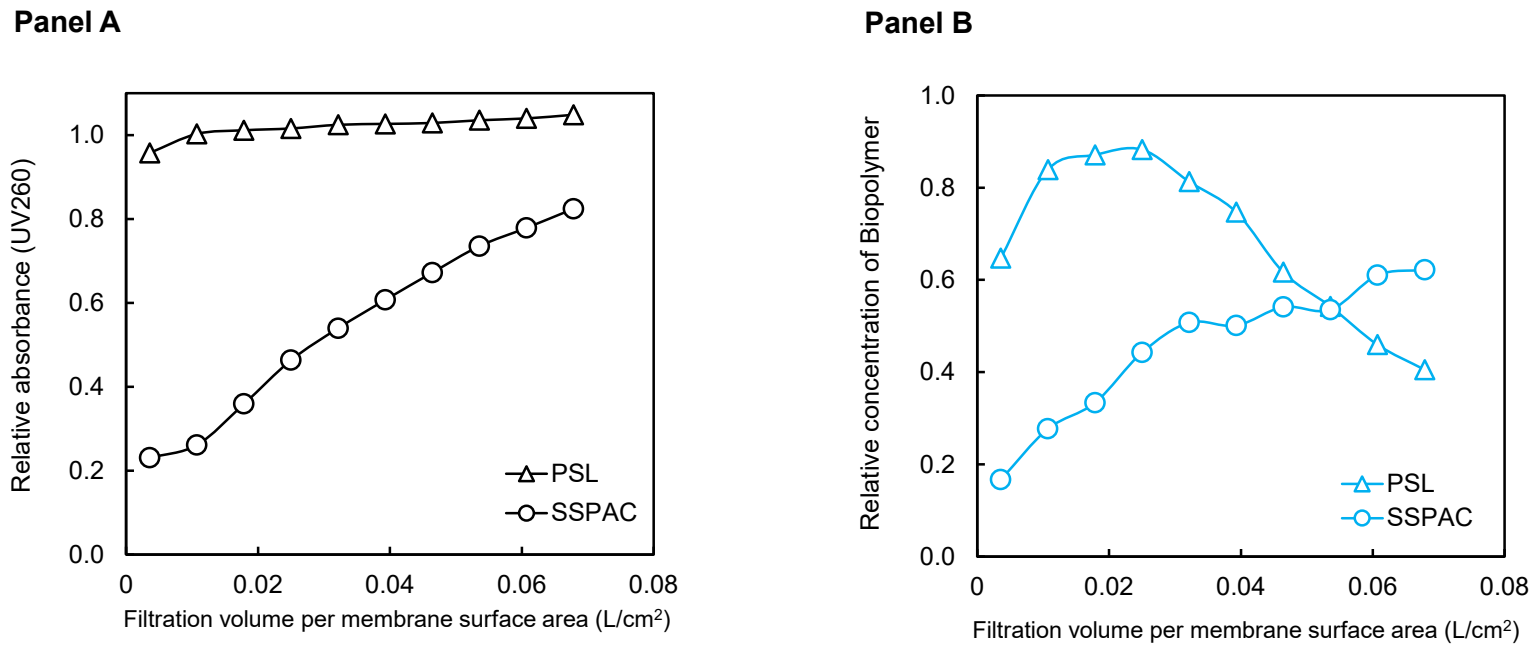

Fig. 17S. Relative absorbance (UV260, Panel A) and relative concentration of biopolymer (Panel B) as a function of filtration volume per membrane surface area. Filtration experiments were conducted by a flat sheet ceramic membrane (Table 3S, SI) with positive pressure. Polystrene latex (PSL) with particle size of 200 nm and SSPAC were used as coating materials. Water-S-3-1 was used in this experiment. Biopolymer concentration in the filtrate from the SSPAC precoat layer increased with time due to the limited adsorption capacity but did not seem to reach the influent concentration level. The PSL precoat layer removed biopolymer though it did not have adsorption capacity. Biopolymer concentration in the filtrate from the PSL precoat layer decreased with time probably due to filter clogging. These results indicate that mechanical separation (straining) is one of the biopolymer removal mechanisms.